UNCLASSIFIED

AD NUMBER
AD025105
CLASSIFICATION CHANGES
TO: **unclassified**
FROM: **confidential**
LIMITATION CHANGES
TO: **Approved for public release; distribution is unlimited.**
FROM: **Distribution authorized to U.S. Gov't. agencies and their contractors; Administrative/Operational Use; MAY 1953. Other requests shall be referred to Office of Naval Research, Washington, DC.**
AUTHORITY
31 May 1965, DoDD 5200.10; .

THIS PAGE IS UNCLASSIFIED

PRELIMINARY DESIGN STUDIES OF A TURBO-RAM-JET MISSILE

PREPARED BY E. K.	AEROPHYSICS DEVELOPMENT CORPORATION	REPORT NO 3002-1-R1
CHECKED BY	PACIFIC PALISADES, CALIFORNIA	DATE: 27 May 1953

Copy No. 54

PRELIMINARY DESIGN STUDIES OF A TURBO-RAM-JET* MISSILE

FINAL REPORT

Contract Number Nonr 897(00)

Task Number NR 094 239

This document contains information affecting the National defense of the United States within the meaning of the Espionage Laws, Title 18, U.S.C., Section 793 and 794. Its transmission or the revelation of its contents in any manner to an unauthorized person is prohibited by law.

*Turbojet with After-burner

Prepared by E. L. Kumm
E. L. Kumm
Project Engineer

and D. Bitondo
D. Bitondo

Approved W. Bollay
W. Bollay

54AA-9908

PREPARED BY E.K.	AEROPHYSICS DEVELOPMENT CORPORATION	REPORT NO. 3002-1-R1
CHECKED BY	PACIFIC PALISADES, CALIFORNIA	DATE 27 May 1953

PRELIMINARY DESIGN STUDIES

OF A

TURBO-RAM-JET MISSILE

FOREWORD

This report was prepared by the Aerophysic Development Corporation under U. S. Navy, Office of Naval Research Contract Number Nonr-897(00). This report consists of work accomplished intermittently during the period October 1952 to the date of this report.

INTRODUCTION

The purpose of the contract under which this work was accomplished was to evaluate in a preliminary fashion the possibilities of using the best presently available turbojet engines with afterburners to power long range missiles.

SUMMARY AND CONCLUSIONS

This report gives results of generalized thermodynamic cycle studies of the turbojet with afterburner. In addition, a more detailed performance analysis is given for a presently available engine to determine what changes are required to make this engine suitable for use in supersonic missiles.

It is concluded that with relatively minor changes in the design, an existing turbojet engine such as the Westinghouse J40-10 could be adapted for use at supersonic flight speeds. The changes required include material changes in the compressor casing, the first four compressor disks and in the accessory arrangement. However, it will not be necessary to change the design of compressor blading, combustion chambers or the turbine. The chief change consists of an afterburner redesigned with a supersonic exit nozzle and a modified fuel control system.

It is concluded that supersonic turbojet missiles have practical advantages over rocket boosted ramjet missiles such as the Navy's Rigel or the Air Force's Navaho II because of the possibility of carrying out an intensive ground development program on the engines and a thorough pre-flight engine check out. This factor does not show up on the performance curves compared to the ramjet but should contribute substantially to an increased reliability of this type of power plant. For example, the J40 engines have been running for several years and are presently being subjected to an intensive development program. By the time a supersonic missile

can be designed and built, these engines should have achieved a high degree of reliability and efficiency.

The preliminary design studies were carried out on typical supersonic missiles for payloads of 4,000 pounds and 8,000 pounds respectively at cruising flight Mach numbers of 2.0 and 2.75. It was concluded that a small, solid propellant rocket weighing about ten percent of the missile weight was desirable to permit zero length take-off. It was found that the supersonic turbojet missiles have a relatively small margin of thrust over drag in the transonic regime. As a result, a missile with a range of 1,650 statute miles would accelerate to a Mach number of 1.0 and an altitude of 35,000 feet in a distance of 40 miles. It would accelerate from Mach number 1.0 to a Mach number of 2.0 at 35,000 feet altitude in a distance of 810 miles. The acceleration and climb then continues from Mach number 2.0 to a Mach number of 2.75 at a total range of 920 miles. The cruise continues at a constant Mach number of M = 2.75 climbing to an altitude of 63,000 feet at its maximum range of 1,650 statute miles. Utilizing J40-10 engines, it was concluded that at least the following missile performance would be achievable.

No. of engines per missile	Initial Weight (Incl. Booster)	Payload	Cruise Mach Number	Cruise Alti-Tude	Range-Statute Miles
Two Engines	84,000 lbs.	8,000 lb.	2.75	63,000 ft.	1650
One Engine	40,000 lbs.	4,000 lb.	2.00	57,000 ft.	1450

In order to achieve the above performance, it is necessary to incorporate the following advanced design features in the missile: a rejectable exhaust nozzle liner, low transonic drag delta wings, an auxiliary two position air scoop intake, and an afterburner fuel control which holds the mechanical rpm constant and allows operation within the compressor map limitations.

The preliminary design studies indicate that a supersonic missile powered by a single turbojet engine is a very promising type for long range Naval applications.

CONTENTS

TABLES

CONFIDENTIAL

PREPARED BY	AEROPHYSICS DEVELOPMENT CORPORATION	REPORT NO. 3002-1-R1
CHECKED BY I.K.	PACIFIC PALISADES, CALIFORNIA	DATE: 27 May 1953

ILLUSTRATIONS

PREPARED BY	AEROPHYSICS DEVELOPMENT CORPORATION	REPORT NO. 3002-1-R1
CHECKED BY E.K.	PACIFIC PALISADES, CALIFORNIA	DATE 27 May 1953

Figure **Page:**

SECTION I

TURBO-RAM-JET ENGINE ANALYSIS

1.1 Introduction

A theoretical analysis was made initially of the performance of turbojet engines with afterburners (turbo-ram-jet) considering a turbine inlet temperature of 1600 degrees F for flight Mach numbers from zero to three at sea level and 35,000'. Three cases were considered in order to clarify the sensitivity of the flight performance factors to the basic operational assumptions. These three cases are labeled, for reference; the Ideal, the Advanced, and the Present engine versions. The flight performance factors consist of the thrust per unit engine frontal area per dynamic head of air (thrust coefficient, C_T) the thrust per pound of air flow (air specific impulse, S_a) and the fuel consumption per hour per pound of thrust (specific fuel consumption, f).

The engine is shown schematically in Figure 1. It consists of a supersonic inlet diffuser, a conventional axial flow compressor, primary combustion chamber, axial flow turbine, an afterburner and a supersonic exit nozzle. The basic assumptions for the versions of the engine are given in Table I. The performance of the Ideal engine cannot be realized, but represents the ultimate possible from this engine cycle with certain exceptions as discussed later. It is believed that the Advanced version

of the engine may be achieved with improvement in components and component efficiencies in perhaps fifteen years from the present. The Present version has components and component efficiencies demonstrated by present day engines of the most developed type.

The Ideal engine assumes a constant characteristic mass flow, X_2, of 30 pounds/sq.ft./sec. of air entering the compressor. Sonic flow conditions give a characteristic mass flow of 49.5 pounds/sq.ft./sec. of air. Thus, the Ideal engine does not assume the maximum air flow possible, but it is believed that it would be difficult to design any compressor that will operate in excess of 30 pounds/sq.ft./sec. characteristic mass flow. The Ideal engine assumes no pressure losses through the engine. The ram pressure recovery is taken quite high over the flight Mach number range (Figure 2). The turbine, compressor, and combustion efficiencies are assumed 100%. The exit nozzle is considered completely variable in size, but the flow is limited in expanding to the maximum turbojet cross sectional area only. The afterburner exit temperature is assumed to be 2500°F, and 3000°F; the case using no afterburner is also calculated.

The Advanced engine assumes optimistically low pressure losses in the primary combustion chamber and in the afterburner. The ram pressure recovery is quite high based on present diffuser tests but may be attainable with future development. More realistic combustion efficiencies are used -- but quite high for the current state of the art. Nevertheless, these combustion efficiencies

should be attainable with new improvements in combustion techniques. Turbine and compressor efficiencies were taken equal to 90% which is also above current practice. A completely variable exit nozzle was used. The Advanced engine like the Ideal assumes a constant characteristic inlet mass flow of 30 pounds/sq.ft./sec.

The Present engine version assumes component performance obtained in current testing of developed engines. Thus the ram pressure recovery is substantially obtainable with a two position inlet diffuser plus an inlet scoop that operates at low Mach numbers only. The turbine, compressor, and combustion efficiencies are being attained or exceeded in current component testing. A fixed exit nozzle is considered for the Present engine designed for a optimum value at Mach number = 2.0, and 35,000 foot altitude for each of the assumed afterburner exit temperatures. The engine characteristic inlet mass flow is held constant at 20. This is exceeded by some current engines at low Mach numbers, but is optimistic at the high Mach numbers used in the cruise phase.

1.2 Analysis Method for Engine

All calculations were based on one-dimensional flow theory using the tables and charts given in Reference 1 and 2. Referring to Figure 1 the flow calculations assumed the gas flow to have the properties of air from station 0 to station 5. However, tables using an isentropic gas exponent of 9/7 was taken for the gas flow through the exit nozzle with afterburner opera-

PREPARED BY E. K.	AEROPHYSICS DEVELOPMENT CORPORATION	REPORT NO 3002-1-R1
CHECKED BY	PACIFIC PALISADES, CALIFORNIA	DATE 27 May 1953

tion. Appendix I gives the derivation of the following equation which relates the engine geometry to the gas flow:

$$(1)\quad \frac{P_0}{p_0}\frac{P_2}{P_0}\frac{P_3}{P_2}\frac{P_4}{P_3}\frac{P_5}{P_4}\frac{P_6}{P_5} = \frac{.00893}{p_0}\frac{A_8}{A_7}\left(1+\frac{w_f}{w_a}\right)\frac{\delta_2}{\sqrt{\theta_2}}\sqrt{T_6}\,X_2\,\frac{\left(1+\frac{\gamma-1}{2}M_7^2\right)^{\frac{\gamma+1}{2(\gamma-1)}}}{\sqrt{\gamma}\,M_7}$$

The left hand side of the above equation is known from efficiencies assumed for the compressor and turbine, and pressure losses assumed in ram compression, the primary combustor and in the afterburner. Thus, for given flight condition the value of

$$\left(1+\frac{w_f}{w_a}\right)\frac{\delta_2}{\sqrt{\theta_2}}\sqrt{T_6}$$

is known and equation (1) becomes

$$(2)\quad \frac{P_6}{p_0} = K_1\frac{A_8}{A_7}X_2\frac{1}{p_0} = K_2$$

From flow tables (Reference 1), the optimum exit area to nozzle throat area is specified by the value of P_6/p_0. The maximum frontal area considered in these calculations is the combustion chamber area so that the optimum exit area is considered equal to or less than the combustion chamber area. Consequently, for high values of P_6/p_0, (such as occurs at high flight speeds) the optimum throat area becomes quite small to obtain maximum flow expansion. If such throat areas were used at high flight speeds, the mass flow passing through the engine is severely restricted (proportional to the throat size) and the available total thrust from even the ideal engine would be small. Consequently, the following

criterion was used for determining the size of the exit nozzle. The area ratio, A_7/A_2, was taken equal to .912. This area ratio gives the maximum value for the total exit thrust in all cases at zero flight Mach number where the exit flow is supersonic and an exit flow gas exponent of 9/7 is used. This area ratio was used on the engine versions providing the resultant characteristic mass flow, X_2, was not larger than the maximum assumed possible for the various engine versions. If the maximum value of X_2 is the limiting consideration, then advantage is taken of the pressure ratio to obtain the greatest exit nozzle velocity by varying the area ratio, A_7/A_2, on the Ideal and Advanced engine versions. It should be realized that the maximum thrust per unit frontal area does not occur at the same exit nozzle area ratio, A_7/A_2, as does the minimum specific fuel consumption. Consequently, the performance curves obtained should be considered as indicative and internally consistent performance data, but individual figures of specific fuel consumption, etc., are not limiting under the assumptions used unless associated with the corresponding thrust coefficient and air specific impulse.

The Present engine version differs from the Advanced and Ideal versions in that the exit nozzle geometry is considered fixed at the optimum value of thrust for $M = 2.0$ and 35,000 feet altitude. Its performance at lower Mach numbers and altitudes is considerably affected by this assumption and this accounts to a significant degree for the relatively poor performance of the Present version

turbojet engine at sea level and zero Mach number. The calculations were based on one square foot of combustion chamber frontal area and the performance characteristics determined as given in Appendix II.

1.3 Generalized Engine Performance

In obtaining the generalized engine performance charts, the compressor was assumed to do constant work per pound of air flow. This has been shown to be a good assumption on actual compressors over a wide range of operation (See Figure 12). This assumes a constant pressure coefficient as follows:

$$\eta_p = \frac{J c_p T_2 \left[\left(P_3/P_2 \right)^{\frac{\gamma-1}{\gamma}} - 1 \right]}{u_b^2/g}$$

It may be perceived that the possible compressor pressure ratio changes as the inlet temperature, T_2, varies. T_2 is a function of the flight Mach number. Figure 3 gives the variation in possible compressor pressure ratio over a range of flight Mach numbers holding the compressor rpm contant. Compressors of higher initial compressor pressure ratios are shown to be more affected by this consideration than those of low initial compressor pressure ratio. Figure 4 gives the characteristic rotor speed versus flight Mach number which indicates that the compressor for the turbojet engine in supersonic flight must operate efficiently over wide limits. Of interest is the engine pressure ratio versus flight Mach number given in Figure 5. The Ideal, Advanced, and Present versions of

the engine give different engine pressure ratios as dependent on the efficiencies and losses assumed in Table I. An engine pressure ratio of one is obtained at M=2.75 for the Present version engine having an initial compressor ratio of 6.0.

Figures 6 and 7 give the generalized performance curves at sea level and 35,000 feet of the turbojet without afterburner. The thrust coefficient of such engines appears quite low at high Mach numbers for the Present version engine and engines having lower design initial compressor pressure ratio show a performance advantage over the higher compressor pressure ratio designs. The performance at 35,000 feet is, of course, better than at sea level due to the lower environmental temperature at altitude. Figures 7 and 8 give the generalized performance curves at sea level and 35,000 feet of the turbojet having an afterburner exit temperature of 2960° R and Figures 9 and 10 are similar to 7 and 8 except that the afterburner exit temperature is 3460° R. It is shown that as the afterburner temperature increases from the no afterburner case to that given in the figures referred to above, that the specific fuel consumption, air specific impulse and thrust coefficient all increase. As an increase in the thrust coefficient is desirable whereas an increase in the specific fuel consumption is undesirable, the choice of operating exit temperature depends on the relative value of the thrust coefficient and the specific fuel consumption. In the trajectory analysis of typical long range flight structures using turbojet engines (Section II of this

report), it was determined that the thrust coefficient was quite critical since it determined whether the missile could pass through the transonic region without excessive reduction of flight weight by fuel consumption. At an exit burner termperature of 3460° R and an altitude of 35,000 feet, these calculations indicate that a turbojet designed for an initial compressor ratio close to four to be optimum. Curves marked 1.0 are also given on the generalized turbojet performance curves of Figures 8, 9, 10 and 11. These are the ramjet performance curves as calculated with the same after-burner exit temperature and an equivalent turbojet engine pressure ratio of 1.0. The turbojet engine appears to have a performance advantage over the ramjet even at high Mach numbers for the 35,000 foot altitude case, though, of course, weighing four to five times as much. However, this conclusion should be accepted with reservation as the ramjet performance calculations were not made using an optimum exit nozzle geometry for the ramjet operation, but rather for the turbojet cases, and in addition, the actual performance of the Present version turbojet decreases at high Mach numbers from that given in the generalized performance curves as discussed in the next portion of this report.

1.4 Present Engine Performance

With the background of information as furnished by the generalized performance calculations, a more detailed analysis was made of an available production type engine to determine its performance and limitations at high Mach numbers and altitudes. It

was determined that the turbine and compressor efficiencies, characteristic mass flow and inlet turbine temperature of one of the large lately developed engines -- the XJ40-10- were essentially the same as those assumed for the Present version turbojet engine. The actual initial compressor pressure ratio of 6.0 is close to the optimum value as calculated in the generalized performance calculations. Discrepancies included the assumed values for the combustion pressure drop, and the combustion efficiency which were taken a little too low. A tabulation of the actual and assumed values for the Present version engine are tabulated in Table II. The overall result of these discrepancies should lower the calculated net thrust and specific fuel consumption somewhat.

Figure 12 gives a compressor map typical of the XJ40-10 engine. The map indicates that characteristic rotor speeds lower than 70% may be easily taken with good operational efficiency with appropriate reductions in the characteristic mass flow. The reductions in characteristic mass flow constitute the only significant difference between the generalized performance curves for the Present version and the actual available engine. This variation is significant enough to warrant a separate calculation of the engine performance over the chosen trajectory. This was accomplished for two cruise Mach number designs, M=2.0 and M=2.75, using actual component efficiencies, pressure losses and the compressor map for this engine as given. The performance characteristics are given in Figure 13.

The operating point for each flight Mach number was selected from the compressor map along the indicated operational line holding the actual RPM of the compressor constant. Thus as the inlet air temperature varied, the characteristic rotor speed, $N/\sqrt{\theta}$, varied as given in Figure 4. The compressor characteristic mass flow, X_2, and compressor pressure ratio for constant RPM are then known. The pressure ratio across the turbine is calculated by equating the turbine work to the compressor work and holding the turbine inlet temperature constant at 1600° by

$$\frac{P_5}{P_4} = \left[1 - \frac{C_{p_{2-3}}}{C_{p_{4-5}}}\frac{T_2}{T_4}\frac{1}{\eta_c \eta_t}\frac{1}{(1+f/a)}\left[\left(\frac{P_3}{P_2}\right)^{\left(\frac{\gamma-1}{\gamma}\right)_{2-3}} - 1\right]\right]^{\left(\frac{\gamma}{\gamma-1}\right)_{4-5}}$$

The compressor efficiency was taken off the compressor map and a constant turbine efficiency of .825 was used. The pressure ratio across the exit nozzle is obtained using the known or assumed pressure drops along the engine by

$$\frac{P_6}{p_0} = \frac{P_0}{p_0}\frac{P_2}{P_0}\frac{P_3}{P_2}\frac{P_4}{P_3}\frac{P_5}{P_4}\frac{P_6}{P_5}$$

A possible error, though small, exists only in P_6/P_5 depending on the exit temperature obtained. Then the throat Mach number is given by

$$\frac{P_6}{p_0} = \left(1 + \frac{\gamma-1}{2}M_7^2\right)^{\left(\frac{\gamma}{\gamma-1}\right)_7}$$

The turbojet gave subsonic exit flow to flight speeds somewhat greater than M=.5. Consequently, the exit nozzle which needed to be a convergent divergent nozzle at cruise Mach numbers of 2.0 and 2.75 was considered to have a light weight refractory liner which held the nozzle throat size constant to the exit (no divergence).

This liner was discarded after a flight speed of M=1.50 was reached. This is believed to be a practical method for the use of a fixed geometry exit nozzle which minimizes the critical exit losses in crucial region of M=1.0. Substitution of the quantities obtained above in the mass flow equation derived in Appendix I allows the determination of $\frac{A_2}{A_7}\sqrt{T_6}$

T_6, the afterburner exit temperature, is chosen for the cruise flight Mach number to give a reasonable thrust coefficient for the engine. This fixes the value of A_2/A_7. For the other flight Mach numbers, A_2/A_7 being fixed, T_6 is calculated. Thus, the engine control contemplated is one which would vary the afterburner fuel flow to hold the engine rpm constant. The variation in the required after burner exit temperature as a function of the flight Mach number is given in Figure 14. The required variation is not severe and only at Mach number = 0 would the afterburner pressure drop be changed from the assumed value. Knowing the pressure ratio across the exit nozzle, the exit velocity may be obtained from one-dimensional flow tables and air specific impulse, specific fuel consumption and thrust coefficient calculated as derived in Appendix II.

The calculations also took into account the additive drag which resulted at off design flight Mach numbers using the theory and figures given in Reference (4). It may be shown that the capture area ratio is related to the flow Mach number and characteristic mass flow as follows:

PREPARED BY E.K.	AEROPHYSICS DEVELOPMENT CORPORATION	REPORT NO 3002-1-R1
CHECKED BY	PACIFIC PALISADES, CALIFORNIA	DATE 27 May 1953

$$\frac{A_0}{A_2} = .0117\, X_2 \frac{P_2}{P_0} \frac{(1+.2M_0^2)^{3.0}}{M_0}$$

Knowledge of A_0/A_2 at the cruise Mach number fixes the value of [illegible]

A_1/A_2 with the result that A_0/A_2 is known for the off design flight Mach numbers. An inlet diffuser cone half-angle of 20° was assumed and the additive drag taken from Figure 7b and 8 of Reference 4. The additive drag losses were not large, not exceeding 5% of the gross thrust coefficient. Thus the performance coefficients given in Figure 13 are independent of the flight structure propelled and are characteristic of the engine with its diffuser and exit nozzle only.

SECTION II

MISSILE TRAJECTORY STUDIES

2.1 Introduction

A study was made of the trajectory of a missile powered by turbojets with afterburners. In order to make a fair comparison of this propulsion system with other long range systems a nearly optimum configuration should be used. The configuration used in this analysis represents recent thinking on long range missile configurations. It is expected that by more careful and extensive design that somewhat better results may be obtained. However, the final configuration considered incorporates all known devices that have been presently considered as being practical solutions to the many problems of high speed supersonic flight. The primary basis for the design of the flight structure lies, of course, in the requirement of obtaining the maximum range for the flight system. During the computation of the drag and the trajectories, the major parameters were observed in order to determine what effect changes would have on the range of the missile system.

The turbojet powered missile has the ability to accelerate from low flight speed to its cruise Mach Number with the same engines. The missile has to be designed so that it will fly at low flight speeds and then accelerate through the transonic region to its cruise flight Mach Number. The wing area is determined from the requirement that it must fly at full load at low subsonic Mach Numbers. However, this wing area is larger then optimum at the

start of cruise. Thus, in order for the missile to fly at its maximum L/D ($\frac{\text{lift}}{\text{drag}}$) ratio it is necessary to have it climb to high altitudes. However, the turbojets with afterburners cannot operate above certain altitudes without flame blowout. Hence, this particular missile was not able to arrive at the altitude where its L/D is maximum. The optimum missile for the cruise would be one that can operate at (L/D) maximum at the maximum ceiling of operation for the engine. However, for the practical missile, this optimum performance must be penalized in order to fly at the low subsonic flight speeds.

2.2 General Arrangement of the Configuration

Two basic configurations were chosen:

1.) A twin engine missile.

2.) A single engine missile.

The assumptions used for the payload and missile elements for each of these missiles is given in Table III . The range for each of the basic configurations was computed for two cruise Mach numbers:

(a) $M = 2.00$

(b) $M = 2.75$

The only changes necessary for change in cruise Mach number were the auxiliary scoop intake areas. The inlet and exhaust nozzle areas were determined from and are consistent with the performance results for the turbo-ram-jet as given in Section I in this report.

The type of missile finally decided upon was a canard

configuration with a 60° swept back delta wing and a nose inlet diffuser on the fuselage. A sketch of this configuration showing the overall dimension is given in Figures 15 and 16. It was assumed in the twin engine configuration that the two engines are placed side by side in the fuselage. The cross sectional shape will then take the form of an ellipse with the major diameter determined from the diameter of the engines. A diameter of 8 feet was ample to house the engines. Assuming a length of 72 feet for the fuselage, this gives a $\frac{\text{length}}{\text{diam.}}$ (for the major diameter of the ellipse) of 9. Previous calculations indicate that such length to diameter ratios give nearly optimum ranges for ducted body missiles. The minor diameter is determined from the volume requirement.

$$D_{minor} = 5.85'$$

The minor diameter was assumed to be 6'.

The duct connecting the diffuser to the engines was assumed to have a diameter of 3-1/3 ft which gave an air velocity of approximately 600 ft/sec at the maximum air flow conditions, and a pressure drop of 0.40 psi (assuming a friction coefficient of 0.01 in the duct).

In the single engine configuration a round fuselage section was assumed. The fuselage length decided on was 59'; and from the volume requirement, the fuselage diameter became 5.20'. A fuselage diameter of 5.60' was actually used.

The 60° swept back wing has a thickness/chord ratio of 0.04 and has its position of maximum thickness 45% back from the

leading edge. The weight of the missile at the start of its flight and after the rocket boost determined the wing area. A wing loading of 90 lbs/ft^2 was used, and it was assumed that the wing carries 80% of the load at the low subsonic Mach numbers. At a Mach number of 0.3 (the start of airborne flight) the lift coefficient is less than 0.6. This value is approximately the maximum lift coefficient allowable from the stability considerations at the subsonic Mach numbers. The above considerations determine the exposed wing areas: (a) for the twin engine configuration - 676 sq. ft., (b) for the single engine configuration - 360 sq. ft. At the supersonic cruise Mach numbers Reference 5 shows that about 75% of the load is carried by the wings. The total area of the control surfaces including the trimmers and fin was calculated to be about 16% of the wing area. The important dimensions of the configurations are shown on Figures 15 and 16.

A sweepback angle of 60° was finally decided upon as it was believed that a larger sweepback would be impractical for three reasons:

1.) Poor characteristics at subsonic speeds.
2.) The wing chord would have to be almost as long as the fuselage.
3.) The drag due to lift is higher.

However, at cruise Mach numbers greater than 2 this wing would necessarily have a sharp supersonic leading edge. The sharp leading edge has two disadvantages:

1.) More difficult to manufacture.

2.) Produces a higher drag due to lift (See Reference 6).

On the other hand, it is not beneficial to increase the sweepback angle of the wing in order to decrease the drag due to lift by the use of a rounded leading edge, as the drag due to lift of the entire wing increases with any increase in the sweepback angle. This is true particularly at high supersonic speeds. Since there was only a small amount of information available on the low subsonic characteristics of delta wings, a compromise angle of 60° was chosen.

A possibly more optimum solution would be to use auxiliary wings during the boost phase, and then at an appropriate point in the missile trajectory discard them while the missile continues on its course using a delta wing whose sweepback is greater and whose area is smaller than the wings shown on Figures 15 and 16. Such a scheme is more complex mechanically and was not considered in this analysis.

Thus, any actual missile, the wing area and sweepback angle are compromised. The lower wing area and larger sweepback angle give a lower $(\frac{L}{D})$ maximum but at the same time the altitude where $\frac{L}{D}$ is maximum is lower. However, the maximum altitude where turbojets with afterburners can operate efficiently, is limited and hence a missile with a large wing area may never be able to fly at the altitude where its $\frac{L}{D}$ is maximum.

2.3 Drag Analysis

The estimation of t he drag, both at zero lift and with

lift, determined the size of propulsion system and thereby, to a large extent, the size of the missile. In order to simplify the procedure for determining the size, two basic configurations were decided upon (see previous subsection) and their sizes determined. Consideration was first given to the drag at zero lift and later to the drag due to lift.

The general procedure that has been followed in making the zero-lift drag estimates is outlined as follows:

Total drag = sum of drag of component parts

Component Drag Determined by:

1. Experimental data.
2. Mixed theory and experimental data.
3. Theory alone.

Pressure Drag Determined on Basis of:

Wings	- projected area
Fins	- exposed area
Cowling	- mixed two and three dimensional flow
Base	- no boattailing

Friction drag calculated by:

Theory - Turbulent Boundary layer - compressible fluid, insulated flat plate

Reynolds Number -
Wings and Fins - maximum exposed chord used
Bodies - axial length used

The pressure drag of the wings was estimated using the total projected wing area through the missile body. It was be-

lieved that this method of computing the wing drag would include interference drag. In all cases where possible, the theoretical calculations were substantiated by experimental results of similar components, and the results were corrected accordingly. Where no experimental results were obtainable, the theoretical values were used as computed.

The wing wave drag was computed by the theory developed by Puckett and others (See References 7, 8, 9, 10, 33 and 34). This was correlated with the experimental results published by N.A.C.A. in many of their Research Memorandum reports (See References 13 to 26 and their bibliographies).

The skin friction coefficients were obtained from the incompressible turbulent skin friction curve of von Karman. For the lower Reynolds numbers a value of 0.0023 for $C_{F\ M=0}$ was obtained from references 11 and 12, both of which gave similar results. A computation of the skin friction drag using the methods of References 23 and 25, checked with the results of the methods mentioned above. The variation of Reynolds number with altitude was taken into account in the computation of the skin friction drag.

The cowling drag on the fuselage was obtained from Reference 9 (page 189).

The base drag coefficient was obtained from Figure 1 of Reference 3. The curve labelled, "Experiment (average) $[Re] = 4 \times 10^6$," was used. The value of this base pressure coefficient is not strictly correct since the missile under consideration has

a jet issuing from the base.

The additive drag is not included in the zero lift curves but is included in the engine performance curves. The additive drag was obtained from References 28 and 29 .

A variable scoop inlet is used during the acceleration phase of the missile in order to supply the engine with sufficient air at the lower Mach numbers. This scoop is closed above M=2.60 for the M=2.75 cruise missile and is closed above M=1.50 for the M=2.00 cruise missile. The drag of this scoop was estimated from the information given in References 11 and 30 . The scoop drag is included in the engine performance curves.

The wing drag due to lift at supersonic speeds ($\frac{\Delta C_D}{C_L^2}$) was largely obtained from Figure 11.36 of Reference 7 . The relation

$$\frac{\Delta C_D}{C_L^2} = \frac{1}{dC_L/d\alpha}$$

was also used to obtain the drag due to lift. References 6 and 23 also give theoretical and experimental values of $\Delta C_D/C_L^2$ which were considered. The above estimates do not include the induced drag due to the control surface force that is necessary to trim the missile at the cruise or flight conditions. The induced drag of the trimmers or canard surfaces can be included in the total drag of the missile in the following way:

$$C_D = C_{D_0} + \frac{\Delta C_D}{C_L^2}(1+K)C_L^2$$

where C_D = total drag coefficient based on projected wing area

C_{D_o} = drag coefficient at zero lift based on projected wing area

$\frac{C_D}{C_L^2}$ = induced drag factor based on projected wing area

K = percentage increase of induced drag factor due to the induced drag of the trimmers.

$$C_M = \frac{L_T \; R}{q S \bar{c}}$$

where C_M = longitudinal moment coefficient about the C. G. point

L_T = Normal aerodynamic force produced by the trimmers

R = Moment arm of trimmer lift forces about the C. G. of missile

S = Projected wing area

$\bar{c}$ = Mean aerodynamic chord

References 13, 14 and 16 give the pitching moment coefficient for several delta wing - body combinations up to a Mach number of 1.80. The curves show that the maximum value of $\frac{dC_M}{dC_L}$ increases with increase in flight Mach number, and at M=1.80, dC_M/dC_L = 0.24. A value of $\frac{dC_M}{dC_L}$ = 0.30 was used to compute the induced drag of the for M=2.0 and M=2.75. Preliminary tests of the North American Aviation XB-64 missile show that it has an approximate value of $\frac{dC_M}{dC_L}$ = 0.13 with attached trimmers. The XB-64 missile is also a canard delta wing configuration, but with side inlets instead of a nose inlet. The above value of 0.30 therefore should be conservative. It is possible to reduce the downwash effects of

the canard surfaces on the main wing by breaking up the vortices by means of vertical fins (perforated or solid) placed at the mid-span of the trimmers. (See Reference 3/). Therefore, the increase of $\frac{dC_M}{dC_L}$ with trimmers deflected could be minimized.

$$\frac{L_T R}{q S \bar{c}} = 0.30\ C_L$$

$$L_T = \frac{0.30\ C_L q S \bar{c}}{R}$$

$$C_{L_T} = \frac{0.30\ C_L}{R} \frac{S\ \bar{c}}{S_T}$$

$$C_{D_i(T)} = \frac{\Delta C_D}{C_L^2}\ C_{L_T}^{\ 2}$$

where S_T = trimmer area

$C_{D_i(T)}$ = trimmer induced drag coefficient based on trimmer area

C_{L_T} = trimmer lift coefficient based on trimmer area

$$C_{D_i\,T(\text{Based on Wing Area})} = \frac{\Delta C_D}{C_L^2}\ C_{L_T}^2\ \frac{S_T}{S}$$

$$C_{D_i}\ (\text{Body \& Wing}) = \frac{\Delta C_D}{C_L^2}\ C_L^2$$

$$C_{D_i}\ (\text{total}) = \frac{\Delta C_D}{C_L^2}\ C_L^2 \left[1 + \frac{S_T}{S} \frac{(.30\ S\ \bar{c})^2}{(R\ S_T)^2} \right]$$

$$C_{D_{i\,(total)}} = \left[1 + \frac{S}{S_T} \frac{(0.30\,\bar{c})^2}{R^2} \right] \frac{\Delta C_D}{C_L^2} C_L^2$$

		TWIN ENGINE	SINGLE ENGINE
S	=	974 sq. ft.	525 sq. ft.
S_T	=	100 sq. ft.	60 sq. ft.
R	=	50 ft.	34 ft.
$\bar{c}$	=	17 ft.	12 ft.
$K = \frac{S}{S_T}\left(\frac{0.30\,\bar{c}}{R}\right)^2$	=	0.101	0.098

The deflected trimmers at cruise then increase the drag due to lift by about 10%. The drag due to lift, plotted against Mach number, is given on Figure 19. This curve showed good agreement with a similar missile designed by an aircraft company.

The curve of (L/D) max. is plotted against Mach number on Figures 20 and 21 for the four cases.

2.4 Trajectory Analysis

The trajectory of the missiles was computed by assuming a typical missile flight path. This flight path consisted of six different phases, as follows:

1. Zero length take-off and acceleration to flying speed ($M = 0.3$) by means of a supplementary rocket boost.
2. Acceleration by means of the turbo-ram-jets to $M = 0.9$
3. Climb to 35,000' altitude at $M = 0.9$
4. Accelerate at 35,000' altitude from $M = 0.9$ to cruise Mach number

5. Climb to maximum altitude at cruise Mach number i.e. where $\frac{L}{D}$ is maximum or maximum ceiling of operation for the turbo-jet whichever is the lowest
6. Cruise at maximum altitude at cruise Mach number

A missile designed for subsonic cruise naturally will have a greater range than a supersonic cruise missile. However, missiles released by the Navy may travel for most of their trajectory over enemy territory, and, consequently, supersonic flight may be necessary to escape detection and interception. The above flight path conforms to supersonic flight adaptable to the turbo-jet engine (See Reference 27).

During the rocket boost phase the missile is allowed to climb along a flight path 10^o to the horizontal. The rocket nozzle is orientated so that the thrust is directed through the missile center of gravity. With this system it is possible to obtain zero length take-off which should be quite desirable for carrier or small field take-off. The rocket thrust for the twin engine configuration is 200,000 lbs with a booster weight of 7,600 lbs. The rocket thrust for the single engine configuration is 100,000 lbs with a booster weight of 4,000 lbs. A specific impulse of 165 was assumed for the propellant.

During the acceleration phases at constant altitude, the trajectory was computed by a step process using the equation

$$m \frac{dv}{dt} = T \cos \alpha - D$$

where m - mass of missile - slugs

v - velocity of missile along flight path - ft/sec

T - Thrust of turbojets - lbs

α - Angle of attack of missile

D - Drag of missile - lbs $\left(C_{D_0} + \frac{\Delta C_D}{C_L^2} C_L^2\right)$

dV/ dt - Acceleration of missile - ft/sec^2

During the climb phases the rate of climb is computed from the following relation

$$\frac{dh}{dt} = \frac{(T-D)\ V}{W}$$

W - weight of missile - lbs

h - altitude - ft

$\frac{dh}{dt}$ - rate of climb - ft/sec

The above methods, while not completely accurate, are sufficiently precise for the present analysis and are much less time-consuming than more exact methods.

In all cases it was found that the missile configuration assumed could not fly at its (L/D) max. since the operation ceiling of present turbojet afterburners limited the cruise altitude. The lift coefficient of the missile was still below the C_L for maximum L/D. The M=2.75 cruise missile could reach and was limited to the 74,000 ft altitude due to the limit on the minimum afterburner static pressure of 8 psi. The M=2.00 cruise missile was

limited to the 57,000 ft altitude. Therefore, after the acceleration to cruise Mach number and climb to these maximum altitudes the missile cruised at constant altitude and Mach number.

For horizontal flight

$$T = D \qquad L = W \quad \text{and} \quad -T = \frac{1}{f}\frac{dW}{dt}$$

$$-T = \frac{1}{f}\frac{dW}{dt} = -D = -Sq\left[C_{D_o} + \frac{\Delta C_D}{C_L^2}\left(\frac{W}{qS}\right)^2\right]$$

Integrating

$$\int_{W_o}^{W_1} \frac{dW}{fSq\left[C_{D_o} + \frac{\Delta C_D}{C_L^2}\left(\frac{W}{qS}\right)^2\right]} = -\int_0^t dt$$

where W_o = missile weight at start of cruise

W_1 = missile weight at end of cruise - empty weight of missile.

Let $fSqC_{D_o} = A$

$$\frac{f}{Sq}\frac{\Delta C_D}{C_L^2} = B$$

Then

$$-t = \int_{W_o}^{W_1}\frac{dW}{A+BW^2} = \frac{1}{\sqrt{AB}}\tan^{-1}\sqrt{B/A}\;W\Big|_{W_o}^{W_1}$$

Range is given by

$$R_a = Vt = \frac{V}{\sqrt{f^2 C_{D_o}\frac{\Delta C_D}{C_L^2}}}\tan^{-1}\sqrt{\frac{\Delta C_D/C_L^2}{C_{D_o}}}\;\frac{W}{Sq}\Bigg|_{W_1}^{W_o}$$

From the parabolic drag polar curve

$$\left(\frac{L}{D}\right)_{max} = \frac{1}{2}\frac{1}{\sqrt{C_{D_o}\frac{\Delta C_D}{C_L^2}}}$$

and
$$(C_L)_{(L/D)max} = \sqrt{\frac{C_{D_o}}{\Delta C_D/C_L^2}} = C_{L_M}$$

$$R_a = \frac{2V}{f}\left(\frac{L}{D}\right)_{max}\left[\tan^{-1}\frac{C_{L_o}}{C_{L_M}} - \tan^{-1}\frac{C_{L_1}}{C_{L_M}}\right]$$

or

$$R_a = \frac{1.36\,V}{f}\left(\frac{L}{D}\right)_{max}\left[\tan^{-1}\frac{C_{L_o}}{C_{L_M}} - \tan^{-1}\frac{C_{L_1}}{C_{L_M}}\right]$$

where f = lbs of fuel per hour per lb. of thrust

v = ft/sec - cruise speed

C_{L_1} - lift coefficient at end of cruise

C_{L_o} - lift coefficient at start of cruise

C_{L_M} - lift coefficient where L/D is maximum

2.5 Results of the Trajectory Studies

The ranges of the four cases were computed by using the above described methods.

It became evident during the calculation of the trajectories that the position of the maximum slope of the zero lift drag curve had a pronounced effect on the results of the trajectories. Actually the important factor was the magnitude of the excess thrust at transonic speeds. The poor performance of the M = 2.75 cruise engine compared to the M = 2.00 cruise engine, was due principally to its lower thrust at the transonic region. The lower performance of the M = 2.75 cruise engine was due to the penalties incurred from the

diffuser and exit nozzles which were designed for optimum operation at M = 2.75. In the M = 2.00 cruise engine these penalties are not as severe.

The results of the trajectories are tabulated below:

	Range	Final Mach Number
Twin Engine M = 2.75 cruise	1658 miles	2.75
Twin Engine M = 2.00 cruise	2020 miles	2.00
Single Engine M = 2.75 cruise	1100 miles	1.18
Single Engine M = 2.00 cruise	1100 miles	1.85
Single Engine M = 2.00 cruise (reduced weight)	1448 miles	2.00

The twin engine configurations gave the better results with the M = 2.00 cruise missile giving the best results. Figure 22 shows the relatively long time that the M = 2.75 cruise missile spends at the transonic Mach numbers compared to the shorter time shown in Figure 23 for the M = 2.00 cruise missile. In both cases the twin engine configurations were able to accelerate through the transonic region.

Neither of the single engine configurations were able to accelerate to their cruise Mach numbers. By flying at a constant Mach number in the transonic speed range, the M = 2.00 cruise missile was able to reach M = 1.85. However, the M = 2.75 cruise missile could not accelerate over M = 1.18. (See Figures 24 and 25)

It was believed therefore that the single engine missile configuration was assumed too large for the engine. A smaller configuration was assumed by reducing the gross weight from 39,200 lbs. to 36,000 lbs. and reducing the wing area from 525 sq. ft. to 484 sq. ft.

The trajectory for the M = 2.0 cruise missile was computed. As shown on Figures 26 and 31, this configuration was able to accelerate to its cruise Mach number and altitude and always had sufficient excess thrust to accelerate although it was marginal in the transonic region. Although the trajectory of the M = 2.75 cruise missile was not computed for the lighter single engine missile, it is believed that better results can be obtained for this configuration also. The variation of time, altitude and Mach number with distance is given in Figures 27 through 31 for each of the configurations.

SECTION III

MODIFICATION AND ADDITIONS REQUIRED OF AVAILABLE ENGINE FOR SUPERSONIC FLIGHT

3.1 General Changes:

The discussion of Section III is directed specifically concerning the Westinghouse XJ40-10 engine, although the same general remarks apply to other similar engines.

The increase in inlet air temperature with an increase in flight Mach number necessitates more severe considerations at M = 2.0 and M = 2.75. However, the required life of components are quite short for a missile application in comparison to more conventional applications. Consequently, components which have been designed to give a reasonable operating life greater than 100 hours at rated rpm and design temperatures are largely sized from stress versus rupture time data. Briefly, this means that for the short time missile applications, the allowable operating temperatures are somewhat higher for most mechanical components. Thus the 12% chromium steel used in the compressor blading may be used for both M = 2.0 and M = 2.75 designs with safety from temperature considerations. Blade growth with increase in inlet temperature is significant, but should not be critical with "wear type" blading. However, the compressor rotor discs should be steel throughout - a portion of them are presently aluminum. The weight differential should not be significant in this change if high strength steel is used with thinner sections. The compressor casing which is presently magnesium need not be changed in

any substantial degree for the M = 2.0 design if the material used is one of the high temperature - high strength cerium alloy magnesiums. For the M = 2.75 design, the casing should be steel due largely to the necessity of retaining strength over temperatures of 500°F to 940°F obtained across the compressor section.

At the higher inlet air temperatures, the primary combustion chamber liner cannot be cooled as effectively and will operate at a higher though not critical temperature. (It appears that the liner would be about 1000°F instead of 500°F). However, the cooling air for the after-burner and exit nozzle must be taken from the inlet before the compressor in the M = 2.75 design during high Mach number operation. Thus, an additional cooling air line with control valve is required on the M = 2.75 design.

A small change is required in the compressor thrust bearing for the M = 2.75 design as the direction of thrust of the rotor system changes when the inlet air temperature is increased sufficiently. This is due chiefly to the decrease in overall engine pressure ratio with flight Mach number as shown in Figure 5.

The position of certain auxiliary apparatus presently on the engine would have to be relocated in the missile due to their present temperature limitation for both M = 2.0 and M = 2.75. The oil cooler and certain electrical apparatus are in this category. These re-locations though troublesome are nevertheless minor in nature.

The general changes referred to above necessitate no major new developments and should be possible to achieve with a minor effort.

3.2 New Engine Developments:

However, there are two new or different developments which require a larger effort.

An afterburner fuel control is indicated that regulates the afterburner fuel to hold the engine rpm constant. The primary combustor fuel should be regulated to hold the turbine exit gas temperature constant. The engineering development work required for such a control appears to be straight forward and should be even less complicated than some of the engine controls now available.

A convergent divergent supersonic exit nozzle is required at the cruise Mach numbers of 2.0 and 2.75. This nozzle must be cooled and equipped with a rejectable refactory liner in the diverging portion. This represents an appreciable new development in terms of time and cost. Again, such a development appears engineeringly feasible though it is evident that a considerable amount of developmental testing must be done.

3.3 Conclusions:

It is believed that an engine such as the Westinghouse XJ40-10 could be adapted in a relatively simple fashion to power long range turbojet missiles of flight Mach numbers of 2.0 and 2.75. Fewer changes are required for the flight M = 2.0 design than the M = 2.75 design, but a new fuel control system and supersonic exit nozzle must be developed for each.

PREPARED BY E. K.	AEROPHYSICS DEVELOPMENT CORPORATION	REPORT NO. 3002-1-H1
CHECKED BY	PACIFIC PALISADES, CALIFORNIA	DATE 27 May 1953

APPENDIX I

DERIVATION OF THE MASS FLOW EQUATION

At the nozzle throat

(1) $$\rho_7 = .0765 \frac{520}{t_7} \frac{P_7}{14.7} = 2.71 \frac{P_6}{T_6} \frac{\left(1+\frac{\gamma-1}{2}M_7^2\right)}{\left(1+\frac{\gamma-1}{2}M_7^2\right)^{\gamma/\gamma-1}}$$

$$\rho_7 = 2.71 \frac{P_6}{T_6} \frac{1}{\left(1+\frac{\gamma-1}{2}M_7^2\right)^{1/\gamma-1}}$$

Also $$v_7 = \sqrt{\gamma g R T_6}\; M_7 \left(\frac{1}{1+\frac{\gamma-1}{2}M_7^2}\right)^{1/2}$$

By continuity of mass flow

(2) $$\rho_7 A_7 v_7 = \omega_a + \omega_f$$

By definition

(3) $$X_2 = \frac{\omega_a}{A_2} \frac{\sqrt{\theta_2}}{\delta_2}$$

Rearranging (2)

(4) $$\rho_7 A_7 v_7 = \left(1+\frac{\omega_f}{\omega_a}\right)\omega_a$$

Substituting for ω_a from (3)

(5) $$\rho_7 A_7 v_7 = \left(1+\frac{\omega_f}{\omega_a}\right)\frac{X_2 \delta_2 A_2}{\sqrt{\theta_2}}$$

Sub.: in (5)

(6) $$\frac{P_6}{P_0} = \frac{.00893}{P_0}\frac{A_2}{A_7}\left(1+\frac{\omega_f}{\omega_a}\right)\sqrt{T_6}\,\frac{\delta_2}{\sqrt{\theta_2}}\,X_2\,\frac{\left(1+\frac{\gamma-1}{2}M_7^2\right)^{\frac{\gamma+1}{2(\gamma-1)}}}{\sqrt{\gamma}\;M_7}$$

PREPARED BY E.K.	AEROPHYSICS DEVELOPMENT CORPORATION	REPORT NO 3002-1-R1
CHECKED BY	PACIFIC PALISADES, CALIFORNIA	DATE 27 May 1953

For $\gamma = 1.30$, $M_7 = 1.0$

$$(7) \quad \frac{P_7}{p_0} = \frac{.0134}{p_0} \frac{A_2}{A_7} \left(1 + \frac{w_f}{w_a}\right) \frac{\delta_2}{\sqrt{\theta_2}} X_2 \sqrt{T_6}$$

or

$$(8) \quad \frac{P_0}{p_0} \frac{P_2}{P_0} \frac{P_3}{P_2} \frac{P_4}{P_3} \frac{P_5}{P_4} \frac{P_6}{P_5} = \frac{.0134}{p_0} \frac{A_2}{A_7} \left(1 + \frac{w_f}{w_a}\right) \frac{\delta_2}{\sqrt{\theta_2}} X_2 \sqrt{T_6}$$

For subsonic exit flow, the exit Mach number must be determined and Equation (8) is

$$\frac{P_0}{p_0} \frac{P_2}{P_0} \frac{P_3}{P_2} \frac{P_4}{P_3} \frac{P_5}{P_4} \frac{P_6}{P_5} = \frac{.00893}{p_0} \frac{A_2}{A_7} \left(1 + \frac{w_f}{w_a}\right) \sqrt{T_6} \frac{\delta_2}{\sqrt{\theta_2}} X_2 \frac{\left(1 + \frac{\gamma - 1}{2} M_7^2\right)^{\frac{\gamma + 1}{2(\gamma - 1)}}}{\sqrt{\gamma}\ M_7}$$

APPENDIX II

EQUATIONS FOR PERFORMANCE CHARACTERISTICS

A. When the base pressure, p_8, exceeds atmospheric pressure, p_o

$$F = m_8 v_8 - m_o v_o + \left(p_8/p_o - 1 \right) p_o \, 144 \, A_8 \qquad (1)$$

$$p_o = 0.172 \sqrt{t_o/520} \; \frac{1}{M_o} \frac{A_2}{A_o} \frac{w_a}{A_2} \qquad (2)$$

Sub. for m_8, m_o, p_o

Air Specific Impulse $(S_a) = \dfrac{F}{w_a} = \dfrac{\left(1 + w_f/w_a\right) v_8}{g} - \dfrac{v_o}{g} + \left(\dfrac{p_8}{p_o} - 1\right) 24.8 \dfrac{A_8}{A_o} \dfrac{A_2}{A_2} \dfrac{1}{M_o} \sqrt{\dfrac{t_o}{520}}$ (3)

Specific Fuel Consumption $(f) = \dfrac{3600}{F/w_a} \dfrac{w_f}{w_a}$ (4)

Thrust Coefficient $(C_T) = \dfrac{F}{q A_2} = \dfrac{F}{w_a A_2} \dfrac{w_a g}{\frac{1}{2} \rho_o v_o^2}$ (5)

$$\rho_o = 2.71 \, p_o/t_o$$
$$v_o^2 = M_o^2 \gamma g R t_o$$
$$w_a = 5.81 \, p_o \frac{A_o}{A_2} \frac{M_o A_2}{\sqrt{t_o/520}} \qquad (6)$$

Sub. for ρ_o, v_o and w_a in (5)

$$C_T = .0575 \frac{F}{w_a} \frac{A_o}{A_2} \frac{1}{M_o} \frac{1}{\sqrt{t_o/520}} \qquad (7)$$

Thrust per Engine $= \dfrac{F}{w_a} A_2 \dfrac{w_a}{A_2} = S_a A_2 X_2 \dfrac{\delta_2}{\sqrt{\theta_2}}$ (8)

B. When the base pressure, p_8, is less than the atmospheric pressure, p_o.

The actual pressure, p_8', at which flow separation actually occurs is obtained from a curve of $\dfrac{p_o - p_8'}{P_6}$ versus

p_8/p_0 for experimental results on rocket nozzles (Ref. 35). Using this correlation, p_8', may be obtained and the ratio p_8'/p_c formed which then determines the area ratio A_8'/A_7 from one dimensional flow tables at the right γ .

$$\text{Base Drag} = (A_8 - A_{8'})\, 144\, p_0 (1 - \eta_{BP})$$

η_{BP} gives the fractional amount of the atmospheric pressure which is present over the base of a high speed body-- generally shown versus the Mach number (Ref. 3)

Using Eq.^n 2 for p_0

$$\frac{\text{Base Drag}}{\omega_a} = 24.8 \frac{A_2}{A_0} \frac{1}{M_0} \sqrt{t_0/520}\, \frac{A_7}{A_2} \left(\frac{A_8}{A_7} - \frac{A_8'}{A_7} \right) \left(1 - \eta_{BP} \right)$$

In addition, there is a pressure thrust loss due to the expansion of the flow to a pressure lower than atmospheric over the nozzle cross sectional area to which the flow expands.

$$\begin{aligned} \frac{\text{Pressure thrust}}{w_a} &= -(p_0 - p_{8'}) A_{8'}\, 144 \\ &= -p_0 (1 - p_8'/p_0) A_{8'}\, 144 \\ &= -24.8 \frac{A_2}{A_0} \frac{\sqrt{t_0/520}}{M_0} \frac{A_8'}{A_2} \left(1 - \frac{p_8'}{p_0} \right) \end{aligned}$$

Sub for p_o

$$S_a = \frac{F}{\omega_a} = \frac{\left(1 + \frac{\omega_f}{\omega_a}\right) v_{8'}}{g} - \frac{v_0}{g} - 24.8 \frac{A_2}{A_0} \frac{\sqrt{t_0/520}}{M_0} \left[\frac{A_8'}{A_2} \left(1 - \frac{p_8'}{p_0} \right) + \frac{A_7}{A_2} \left(\frac{A_8}{A_7} - \frac{A_8'}{A_7} \right) \left(1 - \eta_{BP} \right) \right] \quad (9)$$

The formulas for f and C_T are unchanged.

PREPARED BY E. K.	AEROPHYSICS DEVELOPMENT CORPORATION	REPORT NO 3002-1-R1
CHECKED BY	PACIFIC PALISADES, CALIFORNIA	DATE 27 May 1953

NOMENCLATURE

In Section I And Appendices

Symbols:	Description
A	area, square feet
a	sonic velocity, ft/sec
C_T	thrust coefficient, dimensionless
f	Specific Fuel Consumption, hours^{-1}
F	thrust, pounds
g	acceleration of gravity, ft/sec^2
M_w	molecular weight
M	Mach number, dimensionless
m	mass flow, slugs/sec
n	pressure ratio, dimensionless
P	total pressure, psia
p	static pressure, psia
q	dynamic pressure, psia
R	gas constant $= \frac{1544}{M_w}$
S	impulse, sec.
T	total temperature, ^oR
t	static temperature, ^oR
v	velocity, ft/sec
w	weight flow, pounds/sec
X	characteristic mass flow $= \frac{w\sqrt{\theta}}{A\,\delta}$
γ	isentropic gas exponent, dimensionless
ρ	density, pounds/cu. ft
θ	$T/520$, dimensionless

δ - - - - - - - - - $P/14.7$, dimensionless

η - - - - - - - - - - efficiency

ξ - - - - - - - - - - pressure drop fraction = $\frac{\Delta P}{P}$

Subscripts

0, 1, 2, 3, etc. -- flow station numbers (Fig. 1)

a - - - - air

c - - - - compressor

f - - - - fuel

n - - - - nozzle

t - - - - turbine

BP - - - - base pressure

In Section II
Symbols: Description

A - - - - - - - - - $f S q\, C_{D_0}$

B - - - - - - - - - $\frac{f}{Sq} \frac{\Delta C_D}{C_L^2}$

$\bar{c}$ - - - - - - - - - wing mean aerodynamic chord - ft

C_D - - - - - - - - - total drag coefficient

C_{D_i} - - - - - - - - - induced drag coefficient based on S.

$C_{D_{i(T)}}$ - - - - - - - - trimmer induced drag coefficient based on S_T

C_{D_0} - - - - - - - - - drag coefficient at zero lift based on S

C_F - - - - - - - - - skin friction coefficient based on wetted area

$C_{F_{M=0}}$ - - - - - - - - - incompressible skin friction coefficient

C_L - - - - - - - - - lift coefficient

C_{L_1} - - - - - - - - - lift coefficient at end of cruise

C_{L_0} - - - - - - - - - lift coefficient at start of cruise

PREPARED BY: E. K.	AEROPHYSICS DEVELOPMENT CORPORATION	REPORT NO 3002-1-R1
CHECKED BY:	PACIFIC PALISADES, CALIFORNIA	DATE: 27 May 1953

C_{L_M} - - - - - - - - - lift coefficient where L/D is maximum

C_{L_T} - - - - - - - - - trimmer lift coefficient based on trimmer area

C_M - - - - - - - - - pitching moment coefficient

$$= \frac{\text{pitching moment about center of gravity}}{qS\bar{c}}$$

D - - - - - - - - - drag - lbs

f - - - - - - - - - specific fuel consumption $= \dfrac{\text{lbs fuel}}{\text{hour - lb thrust}}$

h - - - - - - - - - altitude - feet

K - - - - - - - - - increase of induced drag factor $(\Delta C_D/C_L^2)$ due to the induced drag of the trimmers

L_T - - - - - - - - - normal aerodynamic force produced by trimmers

L/D - - - - - - - - - lift-drag ratio

M - - - - - - - - - Mach number

m - - - - - - - - - mass of missile - slugs

R - - - - - - - - - moment arm of trimmer normal forces about the center of gravity of the missile

R_a - - - - - - - - - range - miles

R_e - - - - - - - - - Reynolds number

S - - - - - - - - - wing area - projected - ft^2

S_T - - - - - - - - - exposed trimmer area - ft^2

T - - - - - - - - - thrust - lbs

V - - - - - - - - - missile velocity - ft/sec

W - - - - - - - - - missile weight - lbs

W_0 - - - - - - - - - missile weight at start of cruise

W_1 - - - - - - - - - missile weight at end of cruise - empty weight

$\frac{dh}{dt}$ - - - - - - - - - rate of climb - ft/sec

$\frac{dC_m}{dC_L}$ - - - - - - - - - rate of change of pitching - moment coefficient with lift coefficient

$\frac{\Delta C_D}{C_L^2}$ - - - - - - - - - induced drag factor based on S .

$\frac{dC_L}{d\alpha}$ - - - - - - - - - rate of change of lift coefficient with angle of attack measured at zero lift

α - - - - - - - - - angle of attack

BIBLIOGRAPHY

1. Handbook of Supersonic Aerodynamics, NAVORD 1488 (Vol. 1,2) U. S. Government Printing Office

2. Keenan, J. H. & Kaye, J., Thermodynamic Properties of Air, (1945) John Wiley & Sons, Inc.

3. Chapman, D. R. "An Analysis of Base Pressure at Supersonic Velocities and Comparison with Experiment." NACA TN 2137 (July 1950)

4. Sibulkin, Merwin, "Theoretical and Experimental Investigation of Additive Drag." . NACA RM E51B13, (May 21, 1951) (CONFIDENTIAL)

5. Tucker, Warren A. "A Method for Estimating the Components of Lift of Wing-Body Combinations at Supersonic Speeds." NACA RM L52D22 (Sept. 16, 1952). (CONFIDENTIAL)

6. Osborne, R. S.; Kelly, T. C. "A Note on the Drag due to Lift of Delta Wings at Mach Numbers up to 2.0." NACA RM L53A16a (April 9, 1953)

7. Hilton, W. F. High Speed Aerodynamics, Longmans, Green and Co. New York (1951)

8. Puckett, A. E., "Supersonic Wave Drag of Thin Airfoils." Journal of the Aeronautical Sciences, Vol. 13 No. 9, p. 475 (Sept., 1946)

9. Bonney, E. A., Engineering Supersonic Aerodynamics, McGraw-Hill Books Co., Inc. New York (1950).

10. Ferri, A., Elements of Aerodynamics of Supersonic Flows, The Macmillan Co., New York (1949)

11. Hoerner, S. F., Aerodynamic Drag, S. F. Hoerner 148 Busteed, Midland Park, N. J. (1951)

12. duP Donaldson, Coleman. "On the Form of the Turbulent Skin - Friction Law and its Extension to Compressible Flows." NACA TN 2692 (May 1952).

13. Conrard, Donald. "Lift, Drag and Pitching Moment of Low-Aspect-Ratio Wings at Subsonic and Supersonic Speeds - Plane Triangular Wing of Aspect Ratio 3 with Air-to-Air Missile Models Mounted Externally." NACA RM A52C10a (June 26, 1952) (CONFIDENTIAL)

14. Boyd, J. W., "Aerodynamic Characteristics of Two 25%-Area Trailing-Edge Flaps on an Aspect Ratio 2 Triangular Wing at Subsonic Speeds." NACA RM A52D01c (July 22, 1952). (CONFIDENTIAL)

15. Brown, C. A., Jr.; Bressette, W. E., "Flight Investigation of the Zero-Lift Drag of Two Ram-Jet Missile Configurations at Mach Numbers from 1.00 to 1.89." NACA RM L52J24a (March 9, 1953). (CONFIDENTIAL)

16. Jacobsen, C. R., "Effects of Size of External Store on the Aerodynamic Characteristics of an Unswept and a 45° Sweptback Wing of Aspect Ratio 4 and a 60° Delta Wing at Mach Numbers of 1.41, 1.62 and 1.96." NACA RM L52K20a (Jan. 21, 1953). (CONFIDENTIAL)

17. Whitcomb, R. T., "A Study of the Zero-Lift Drag-Rise Characteristics of Wing-Body Combinations near the Speed of Sount." NACA RM L52H08 (Sept. 3, 1952) (CONFIDENTIAL)

18. Leiss, Abraham "Flight Measurements at Mach Numbers from 1.1 to 1.9 of the Zero-Lift Drag of a Twin-Engine Supersonic Ram-Jet Configuration." NACA RM L52D24 (June 23, 1952) (CONFIDENTIAL)

19. Morrow, J. D.; Nelson, R. L., "Large-Scale Flight Measurements of Zero-Lift Drag of 10 Wing-Body Configurations at Mach Numbers from 0.8 to 1.6." NACA RM L52D18(a) (Jan. 15, 1953) (CONFIDENTIAL)

20. Smith, Willard G., "Wind-Tunnel Investigation at Subsonic and Supersonic Speeds of a Model of a Tailless Fighter Airplane Employing a Low-Aspect-Ratio Swept-Back Wing." NACA RM A52J31 (Jan. 12, 1953) (CONFIDENTIAL)

21. Hasel, L. E.; Sinclair, A. E.; Hamilton, C. V., "Preliminary Investigation of the Drag Characteristics of the NACA RM-10 Missile at Mach Numbers of 1.40 and 1.69 in the Langley 4 by 4 Foot Supersonic Tunnel." NACA RM L52A14 (April 18, 1952)

22. Nielson, J. N., Kaattari, G. E., Drake, W.C., "Comparison between Prediction and Experiment for All-Movable Wing and Body Combinations at Supersonic Speeds - Lift, Pitching Moment, and Hinge Moment," NACA RM A52D29 (Aug. 8, 1952) (CONFIDENTIAL)

23. Katzen, E. D.; Kaattari, G. E., "Drag Interference between a Pointed Cylindrical Body and Triangular Wings of Various Aspect Ratios at Mach Numbers of 1.50 and 2.02." NACA RM A51C27 (May 23, 1951) (CONFIDENTIAL)

24. Mitcham, G. L.; Crabill, N. L.; Stevens, J. E., "Flight Determination of the Drag and Longitudinal Stability and Control Characteristics of a Rocket-Powered Model of a 60° Delta-Wing Airplane from M = 0.75 to M = 1.70." NACA RM L51I04 Nov. 29, 1951 (CONFIDENTIAL)

25. Vincenti, W. G.; Nielsen, J. N.; Mateson, F. H., "Investigation of Wing Characteristics at a Mach Number of 1.53. I - Triangular Wings of Aspect Ratio 2." NACA RM A7 I 10 (Dec. 19, 1947) (CONFIDENTIAL)

26. Nielsen, J. N. Katjen, E. D., Zang, K. K. "Lift and Pitching - Moment Interference between a Pointed Cylindrical Body and Triangular Wings of Various Aspect Ratios at Mach Numbers of 1.50 and 2.02." NACA RM A50 F 06 (Sept. 12, 1950) (CONFIDENTIAL)

27. Hall, E. W.; Henneberry, H. M.; Evans, P. J., Jr., "Analysis of Missile Propulsion Systems", NACA Conference on Supersonic Missile Propulsion (March 13, 1952) (CONFIDENTIAL)

28. Wyatt, DeM. D., "Aerodynamic Force Associated with Inlets of Turbojet Installations." Aeronautical Engineering Review, Vol. 10, No. 10, Page 20 (October 1951)

29. Sibulkin, M., "Theoretical and Experimental Investigation of Additive Drag." NACA RM E 51 B13 (May 21, 1951) (CONFIDENTIAL)

30. Graham, E. W., "Notes on the Drag of Scoups and Blunt Bodies." Report No. SM-13474 Douglas Aircraft Co., Inc. (April 13, 1950)

31. Wise, G. A., "Influence of End-Plates on Lift and Flow Field of a Canard-Type Control Surface at Mach number of 2.00." NACA RM E53 A02 (March 23, 1953) (CONFIDENTIAL)

32. Pepper, W. B., Jr.; Hoffman, S., "Transonic Flight Tests to Determine the Effect of Thickness Ratio and Plan-Form Modification on the Zero-Lift Drag of a 45° Sweptback Wing." NACA RM L52 F02a (August 12, 1952) (CONFIDENTIAL)

33. Lawrence, T., "Charts of the Wave Drag of Wings at Zero Lift" Technical Note No. AERO 2139 Royal Aircraft Establishment England (Jan, 1952)

34. Weber, J.; Brebner, G. G., "A Simple Estimate of the Profile Drag of Swept Wings", Technical Note No. AERO 2168 Royal Aircraft Establishment, England (June 1952) (CONFIDENTIAL)

35. Green, Leon, Jr., "Flow Separation in Rocket Nozzles" Journal of the American Rocket Society, (Jan.-Feb. 1953) (pg. 34-35

PREPARED BY E.K.	AEROPHYSICS DEVELOPMENT CORPORATION	REPORT NO. 3002-1-R1
CHECKED BY	PACIFIC PALISADES, CALIFORNIA	DATE 1/20/53

TABLE I

OPERATIONAL FACTORS ASSUMED FOR THE TURBO-RAMJET

Versions	Mach. No.	X	P_2/P_0	η_c	η_t	η_n	$\eta_{f_{3-4}}$	$\eta_{f_{5-6}}$	ξ_{3-4}	ξ_{5-6} $T_6=2500°F$	ξ_{5-6} $T_6=3000°F$	ξ_{5-6} No AB	$C_{[illegible]}$
Ideal	0	30	1.0	100	100	100	100	100	0	0	0	0	1.0
	1	30	.95	100	100	100	100	100	0	0	0	0	1.0
	2	30	.85	100	100	100	100	100	0	0	0	0	1.0
	3	30	.60	100	100	100	100	100	0	0	0	0	1.0
Advanced	0	30	.90	90	90	97.5	95	90	.03	.04	.06	0	1.0
	1	30	.95	90	90	97.5	95	90	.03	.04	.06	0	.8
	2	30	.85	90	90	97.5	95	90	.03	.04	.06	0	.6
	3	30	.55	90	90	97.5	95	90	.03	.04	.06	0	.4
Present	0	20	.90	82.5	82.5	97.5	95	80	.04	.05	.08	.02	1.0
	1	20	.925	82.5	82.5	97.5	95	80	.04	.05	.08	.02	.8
	2	20	.85	82.5	82.5	97.5	95	80	.04	.05	.08	.02	.6
	3	20	.50	82.5	82.5	97.5	95	80	.04	.05	.08	.02	.4

Note: Combustion efficiencies are based on the ratio of the actual (f/a) to the theoretical (f/a) to achieve a specified temperature increase for constant pressure combustion.

PREPARED BY E.K.	AEROPHYSICS DEVELOPMENT CORPORATION	REPORT NO 3002-1-R1
CHECKED BY	PACIFIC PALISADES, CALIFORNIA	DATE 27 May 1953

TABLE II

OPERATIONAL FACTORS OF THE

PRESENT VERSION TURBO-JET

	Assumed Value	Test Value Obtained
X_2	20	20.1
η_c	82.5%	82.0%
η_t	82.5%	81.7%
η_n	97.5%	95.0%
$\eta_{\xi 3-4}$	95%	97.0%
$\eta_{\xi 5-6}$	80%	88%
ξ_{3-4}	.04	.07
$\xi_{5-6}^{T_t=3000^\circ F}$	.08	.15

Note: at zero Mach number

TABLE III

MISSILE VOLUME & WEIGHT REQUIREMENTS

Components	Missile Type	
	Twin Engine	Single Engine
Warhead	8000 lbs	4000 lbs
Guidance	2500 lbs	2000 lbs
Turbojets	8400 lbs	4200 lbs
Structural (including fuel tanks)	6500 lbs	3000 lbs
Empty Weight	25400 lbs	13200 lbs
Fuel	51000 lbs	26000 lbs
Flying Weight	76400 lbs	39200 lbs
Rocket Booster	7600 lbs	4000 lbs
Total Take-off Weight	84000 lbs	43200 lbs

Warhead	250 cu.ft.	125 cu.ft.
Diffuser	375 cu.ft.	150 cu.ft.
Engines	625 cu.ft.	315 cu.ft.
Fuel	990 cu.ft.	505 cu.ft.
Air Duct	350 cu.ft.	140 cu.ft.
Guidance	60 cu.ft.	50 cu.ft.
Total Volume of Fuselage	2650 cu.ft.	1285 cu.ft.

PREPARED BY K.H.J.	AEROPHYSICS DEVELOPMENT CORPORATION	REPORT NO 3002-1-R1
CHECKED BY E.K.	PACIFIC PALISADES, CALIFORNIA	DATE 1/10/53

FIG. 1

THE TURBO-RAMJET

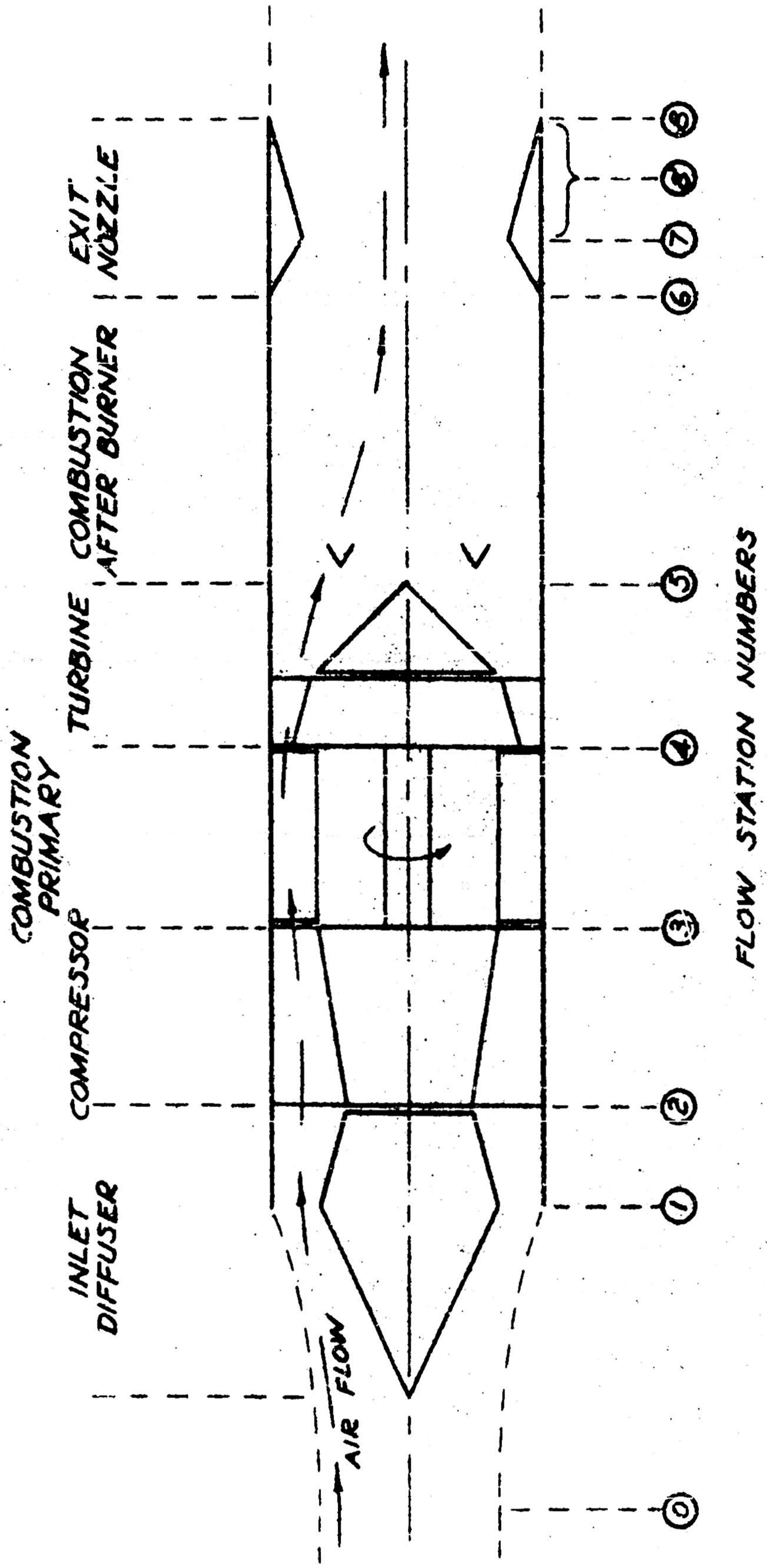

PREPARED BY: E. K.	AEROPHYSICS DEVELOPMENT CORPORATION	REPORT NO: 3002-1-R1
CHECKED BY:	P. O. BOX 657, PACIFIC PALISADES, CALIFORNIA	DATE: 1/10/53

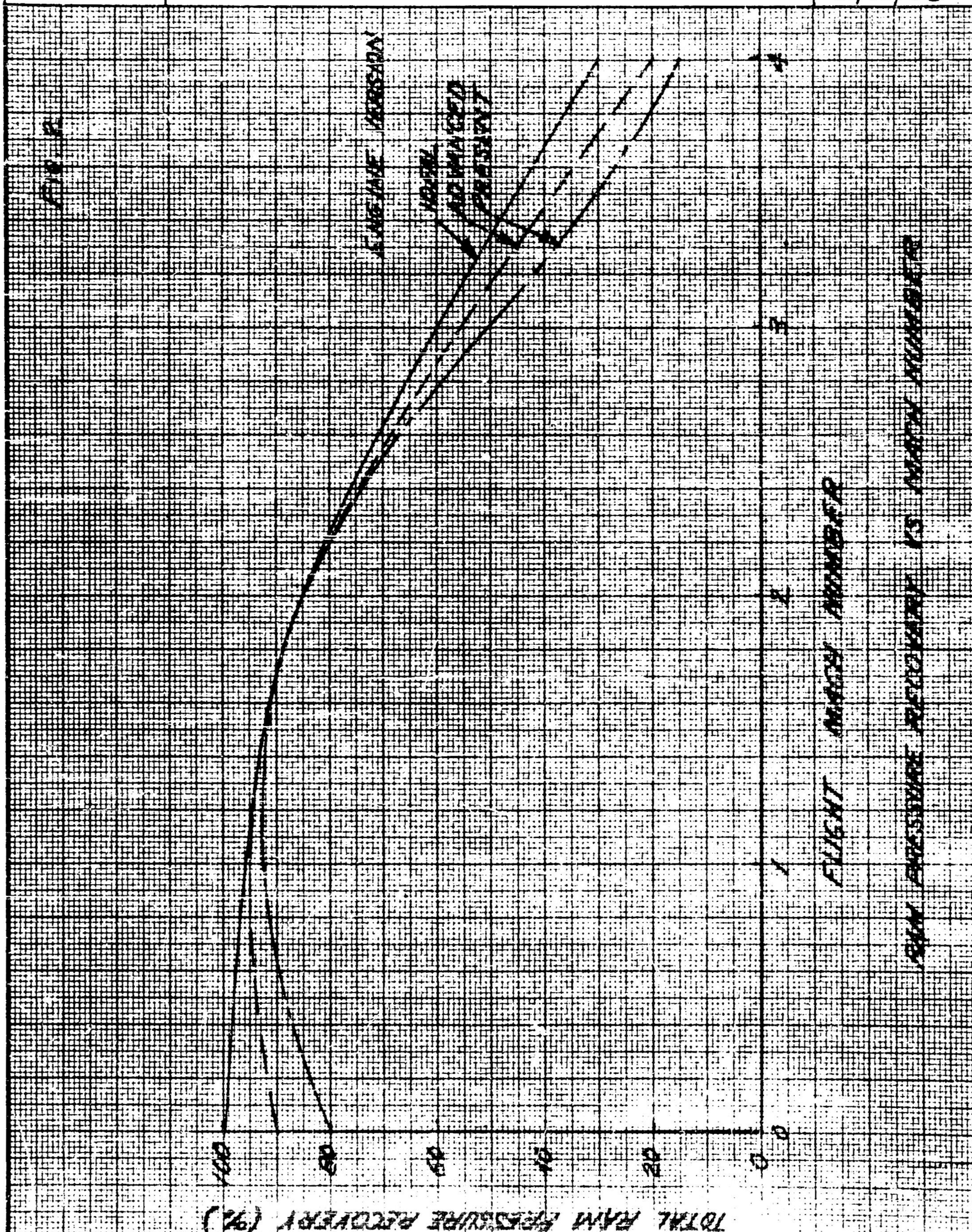

CONFIDENTIAL

PREPARED BY: E. K.	AEROPHYSICS DEVELOPMENT CORPORATION	REPORT NO: 3002-1-R1
CHECKED BY:	P. O. BOX 657, PACIFIC PALISADES, CALIFORNIA	DATE: 3/16/53

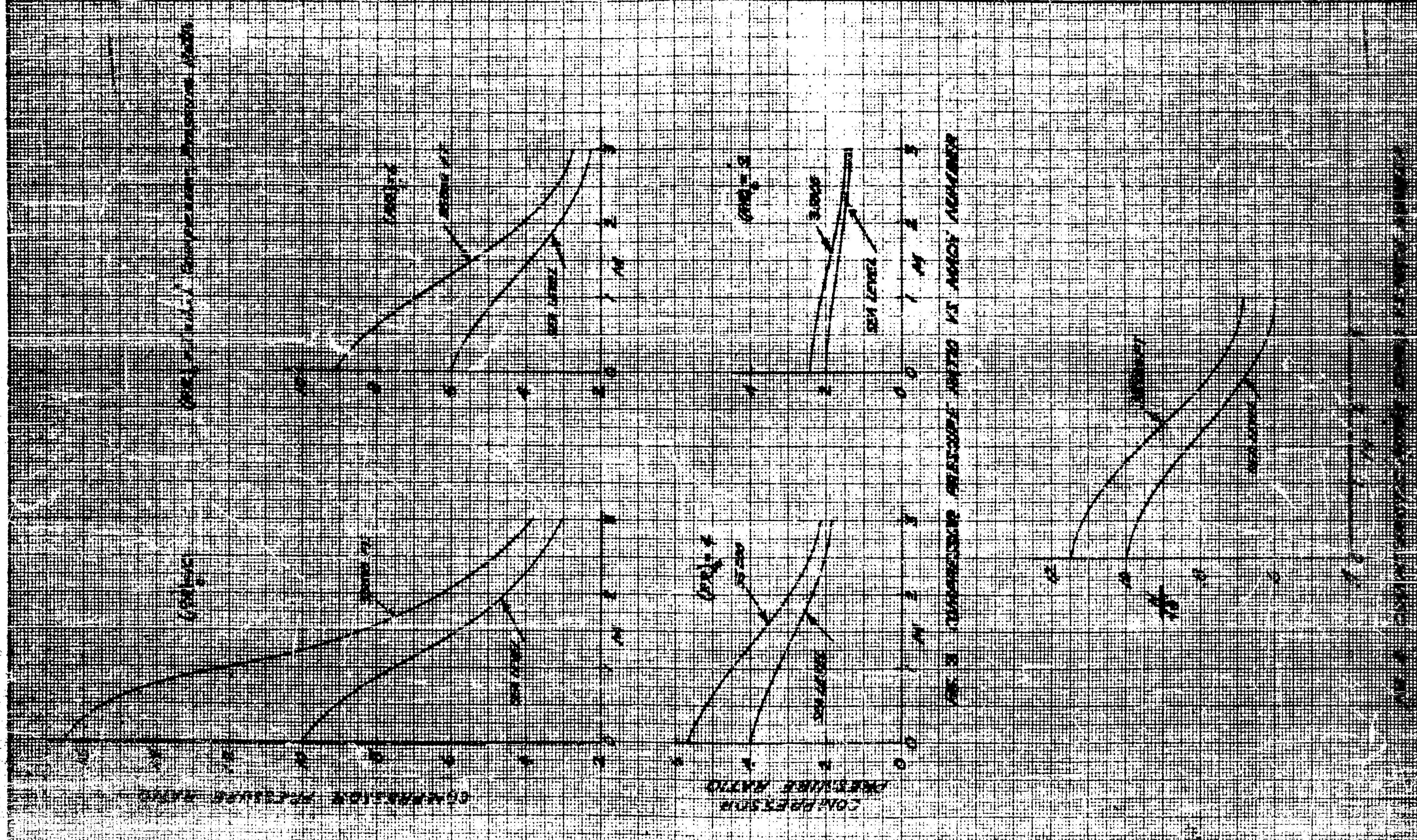

CONFIDENTIAL

CONFIDENTIAL

PREPARED BY: BC	AEROPHYSICS DEVELOPMENT CORPORATION	REPORT NO. 9002-1-R1
CHECKED BY: E.K.	P.O. BOX 657, PACIFIC PALISADES, CALIFORNIA	DATE: 5-53

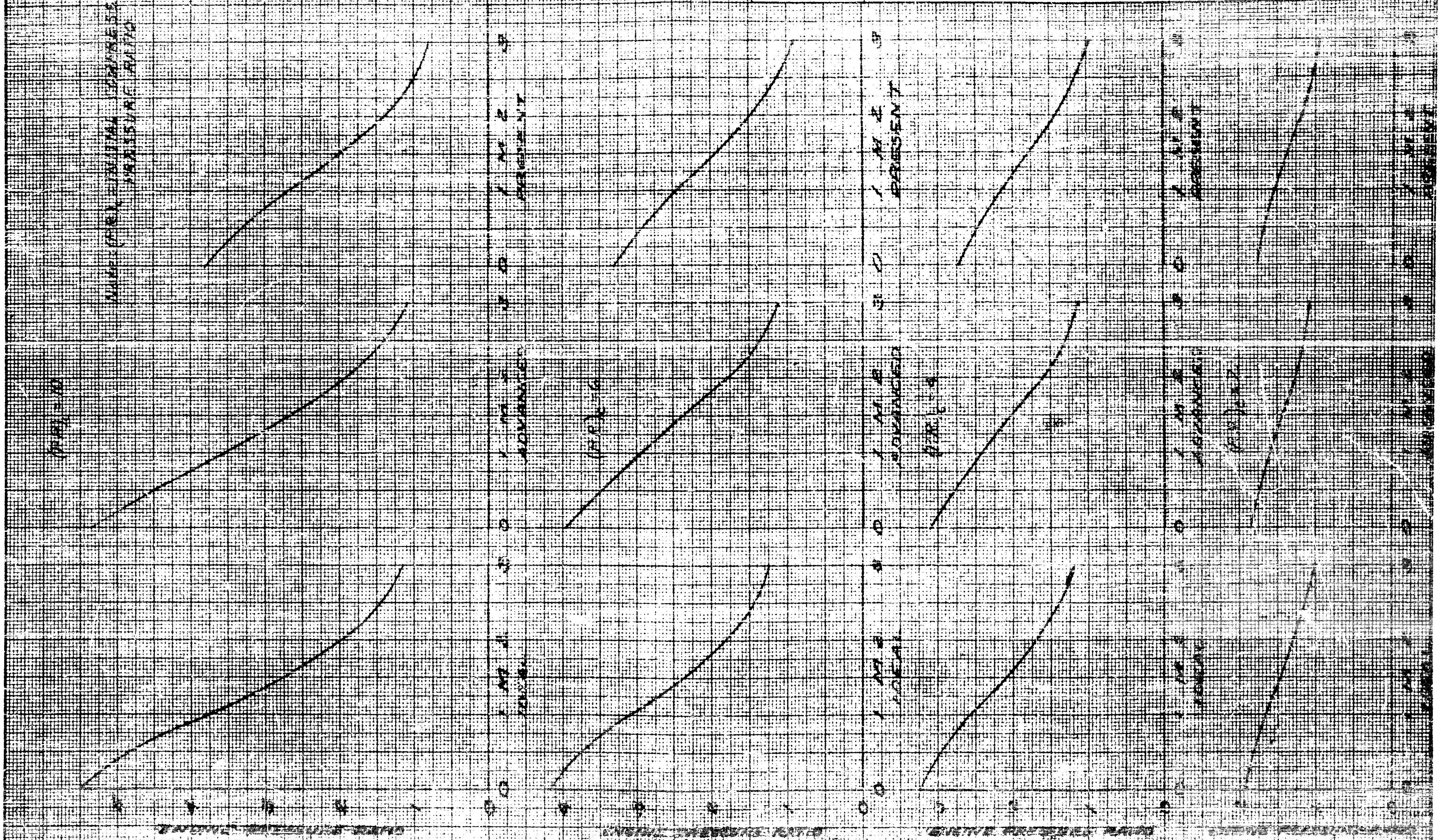

FIG 5 ENGINE PRESSURE RATIO VS FLIGHT MACH NO.

CONFIDENTIAL

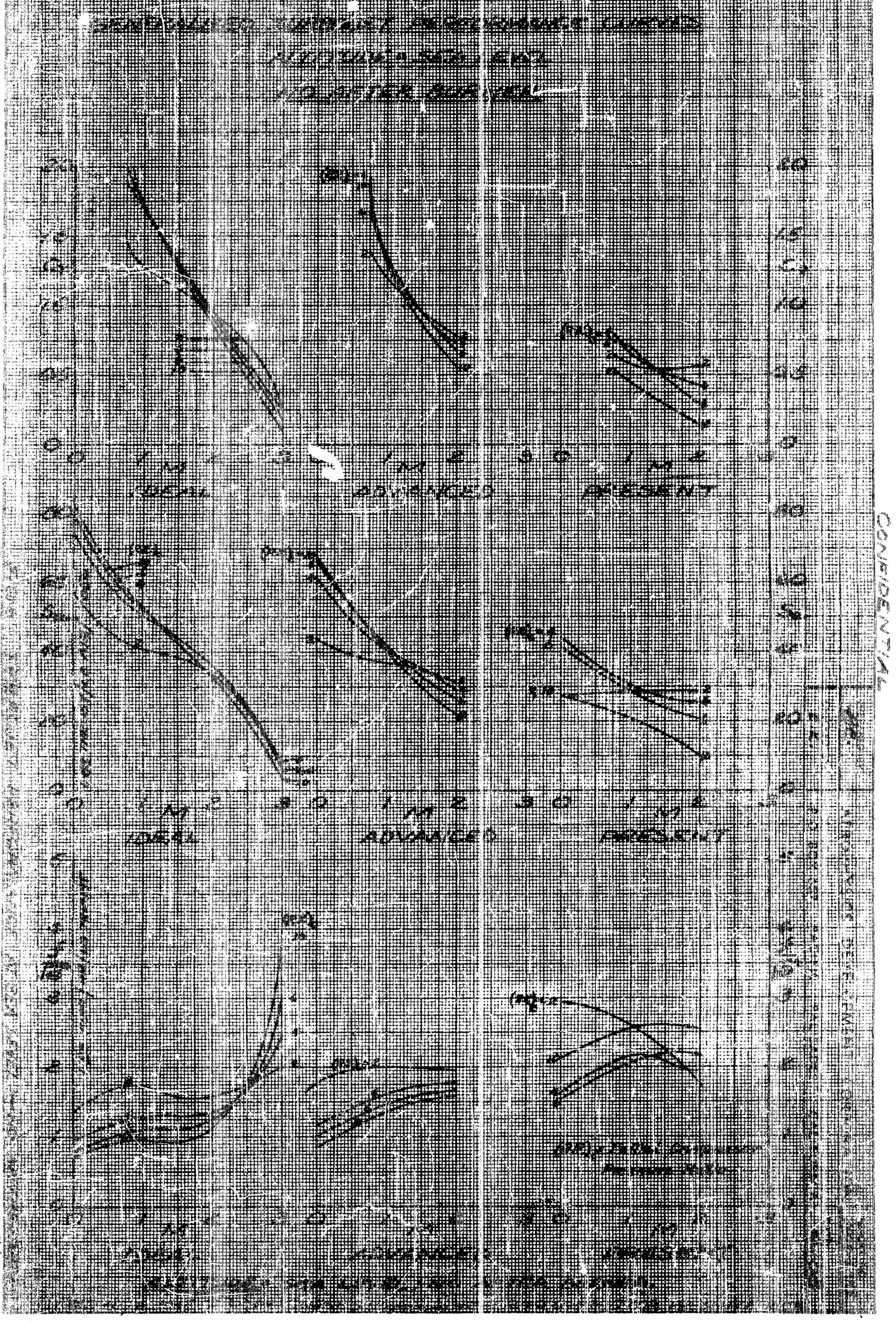
PERFORMANCE CURVES
IDEAL
ADVANCED
PRESENT
M
IDEAL
ADVANCED
PRESENT
M
CONFIDENTIAL

CONFIDENTIAL

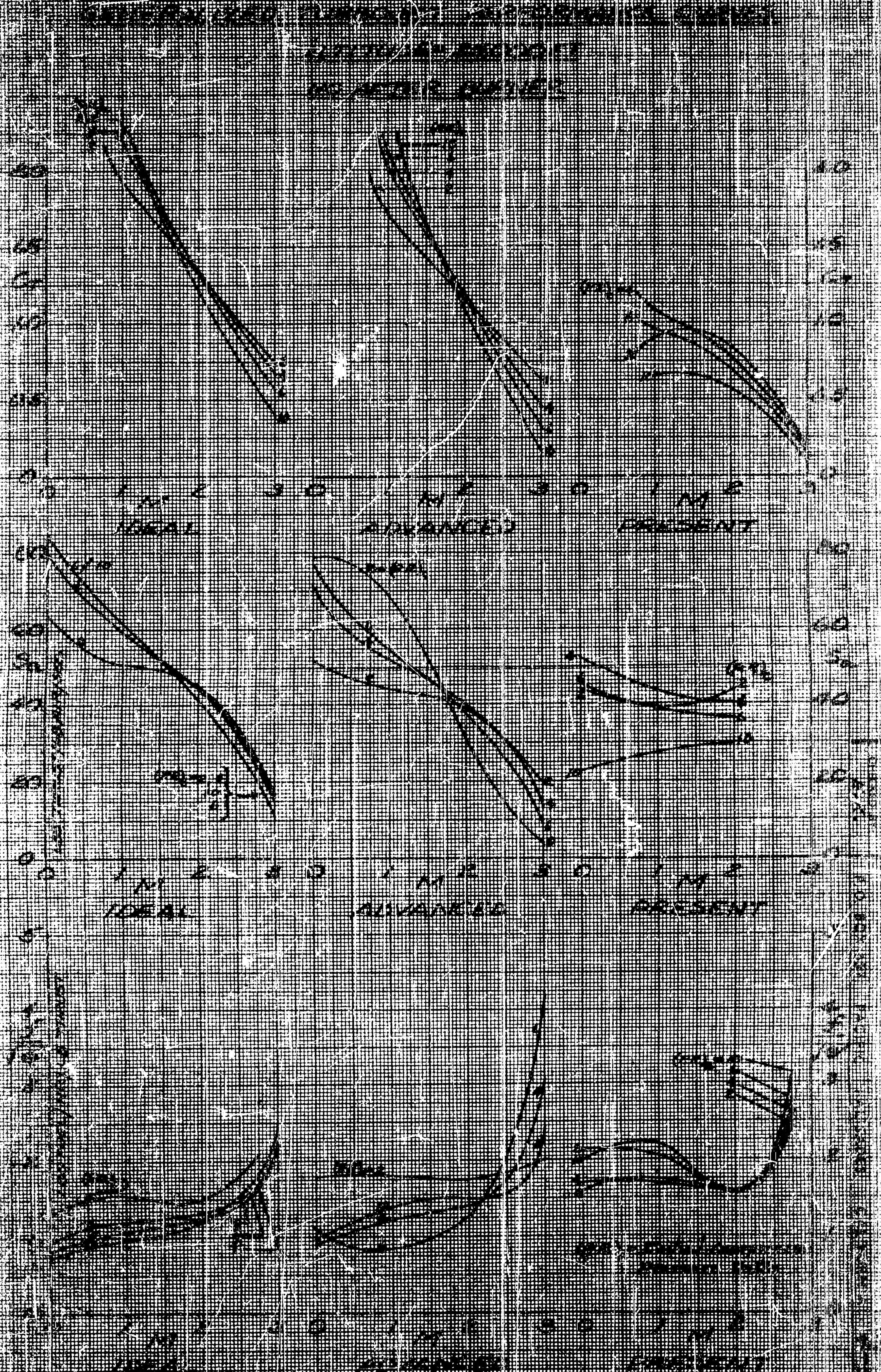

CONFIDENTIAL

CONFIDENTIAL

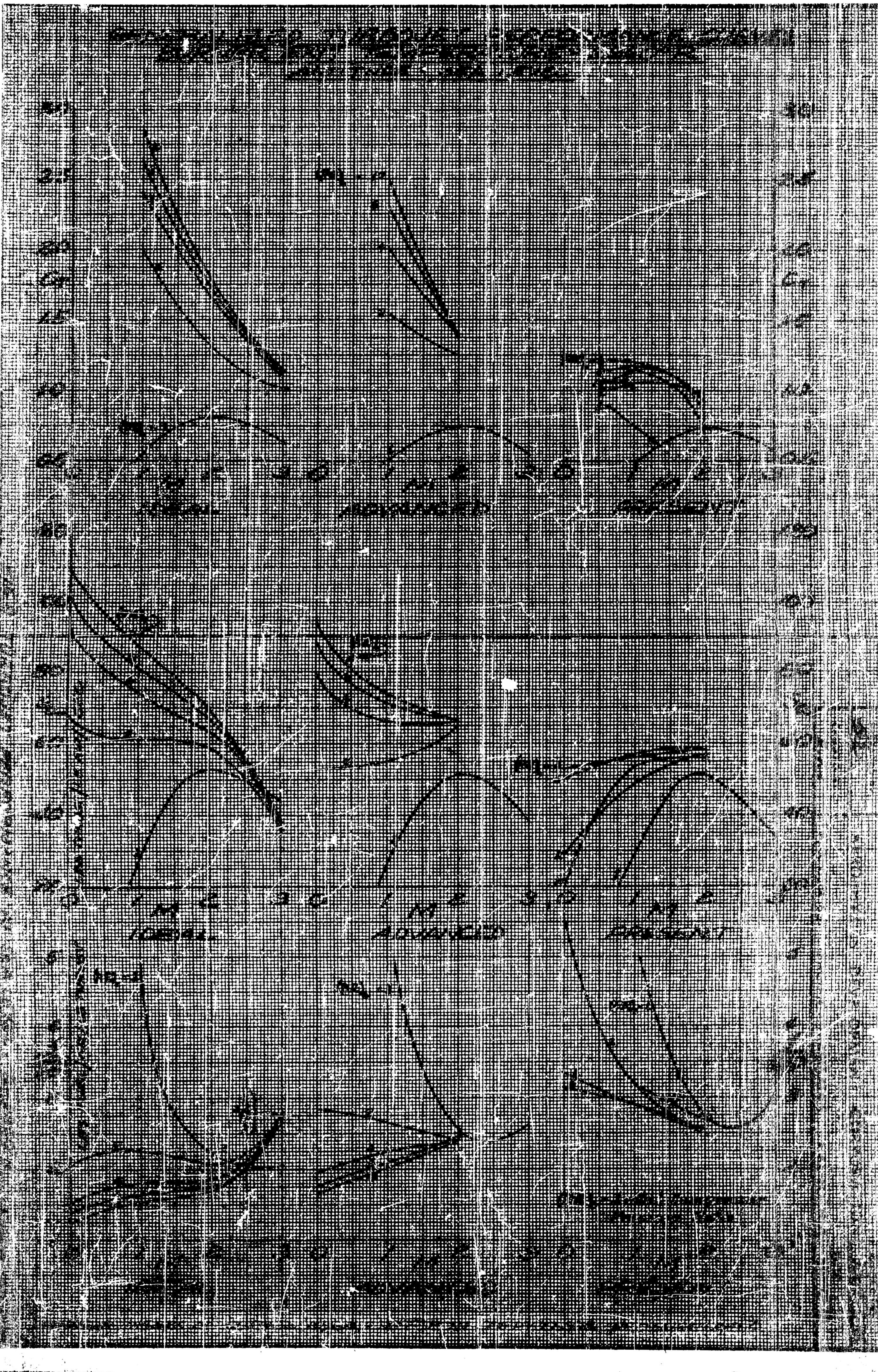

CONFIDENTIAL

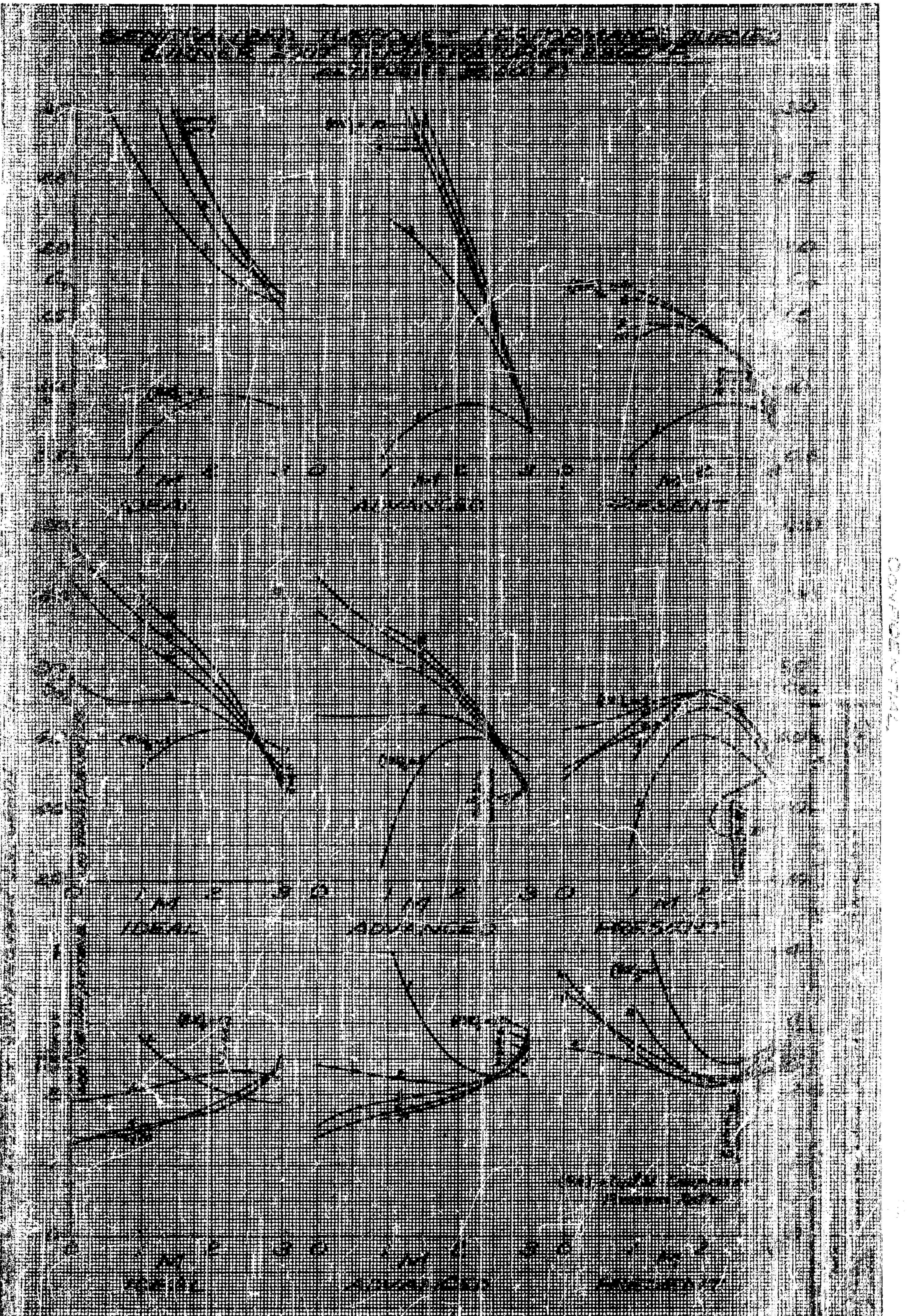
IDEAL
ADVANCED
PRESENT
IDEAL
ADVANCED
PRESENT
IDEAL
ADVANCED
PRESENT

M
IDEAL
ADVANCED
PRESENT
CONFIDENTIAL

CONFIDENTIAL

PREPARED BY: E.K.	AEROPHYSICS DEVELOPMENT CORPORATION	REPORT NO: 3002-1-R1
CHECKED BY:	P.O. BOX 657, PACIFIC PALISADES, CALIFORNIA	DATE: 5/22/53

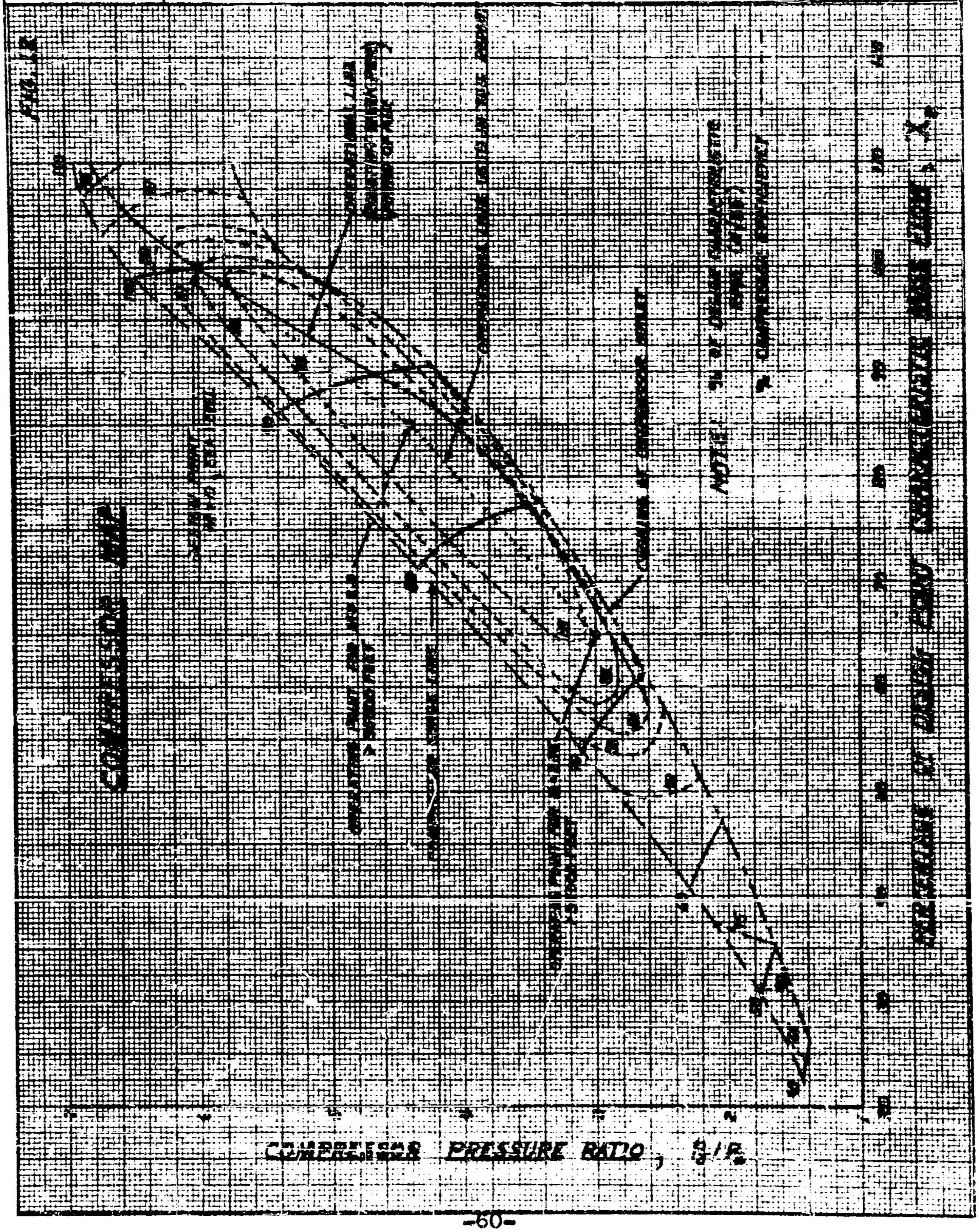

PREPARED BY: E.K.	AEROPHYSICS DEVELOPMENT CORPORATION	REPORT NO: 3002-1-R1
CHECKED BY:	PACIFIC PALISADES, CALIFORNIA	DATE: 5/23/53

FIG. 13

PERFORMANCE CHARACTERISTICS OF ACTUAL ENGINE

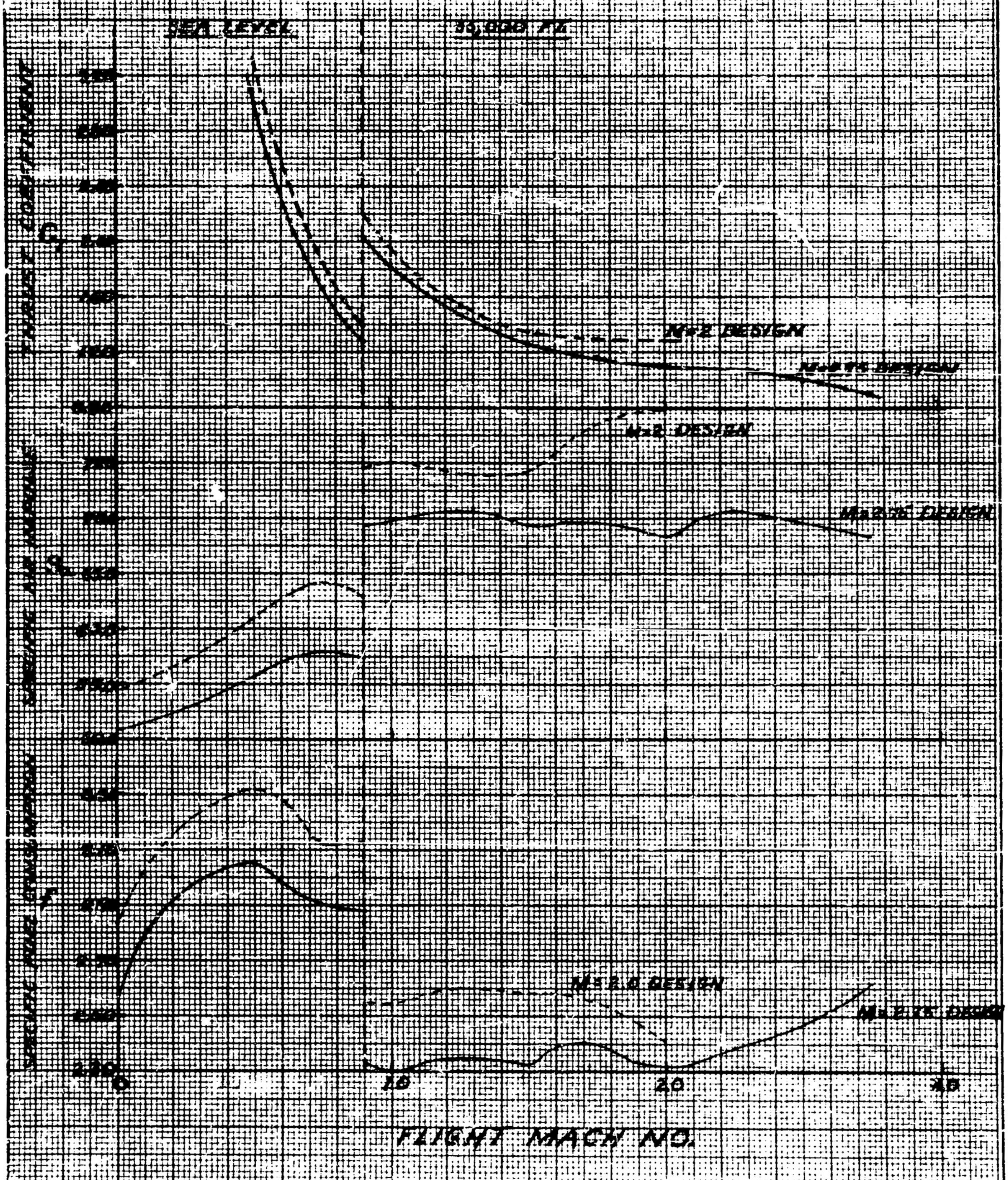

PREPARED BY: E. K.	AEROPHYSICS DEVELOPMENT CORPORATION	REPORT NO: 3002-1-R1
CHECKED BY:	P. O. BOX 657, PACIFIC PALISADES, CALIFORNIA	DATE: 5/23/53

FIG. 14

AFTERBURNER EXIT TEMPERATURE

VERSUS

FLIGHT MACH NUMBER

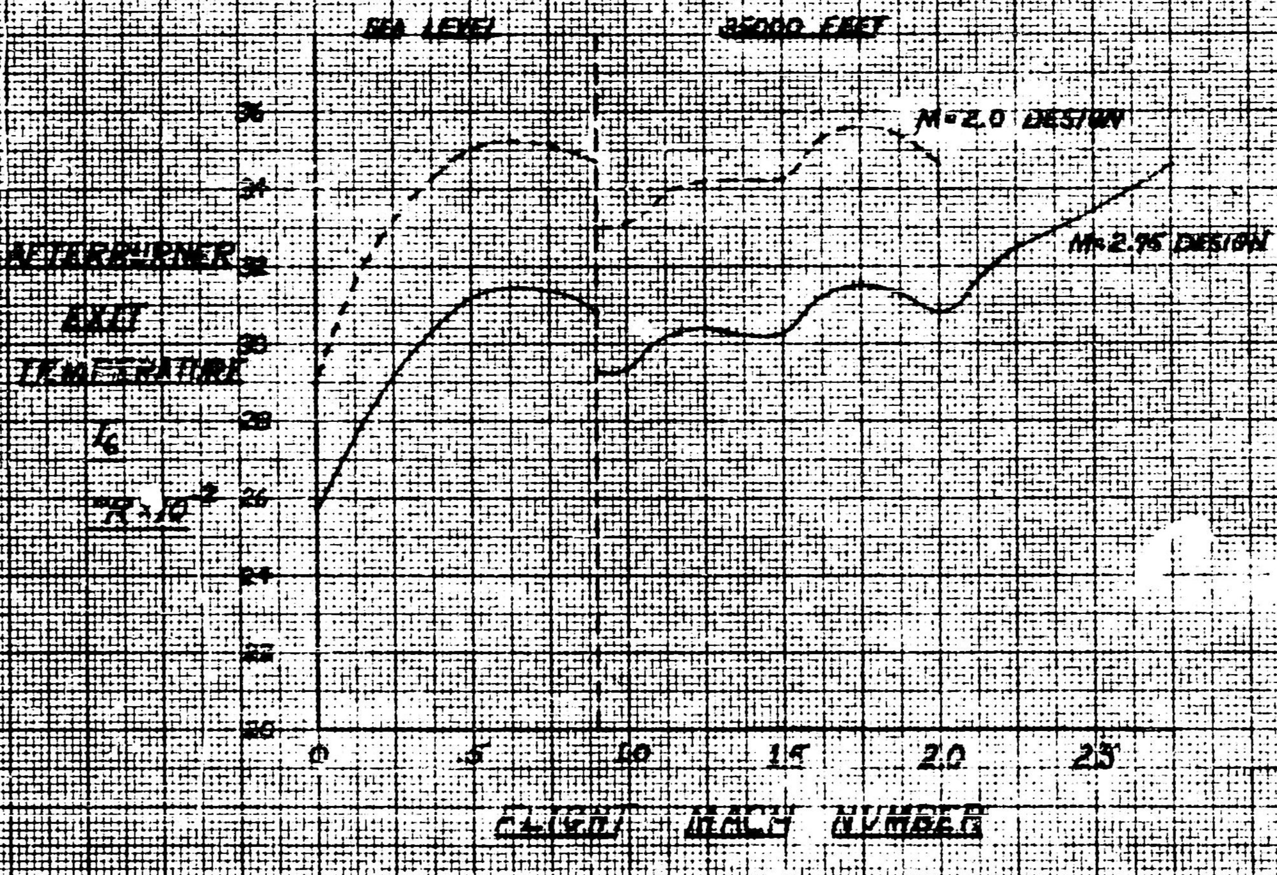

PREPARED BY H.S.	AEROPHYSICS DEVELOPMENT CORPORATION	REPORT NO 3002-1-R1
CHECKED BY DB	PACIFIC PALISADES, CALIFORNIA	DATE: 27 May 1953

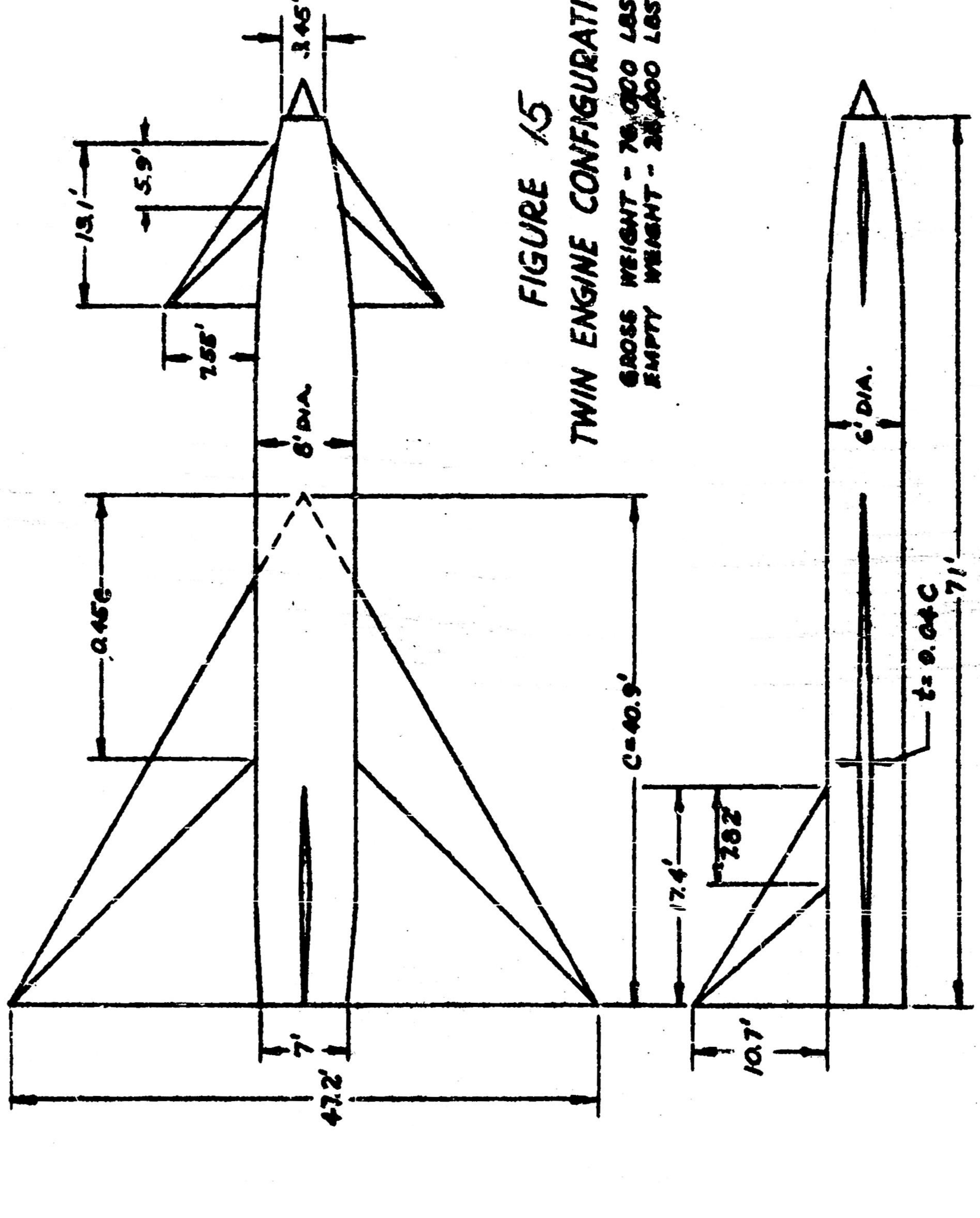

FIGURE 15
TWIN ENGINE CONFIGURATION

GROSS WEIGHT - 76,000 LBS.
EMPTY WEIGHT - 2[illegible],000 LBS.

PREPARED BY: H.S	AEROPHYSICS DEVELOPMENT CORPORATION	REPORT NO. 3002-1-R1
CHECKED BY: RB	PACIFIC PALISADES, CALIFORNIA	DATE 27 May 1953

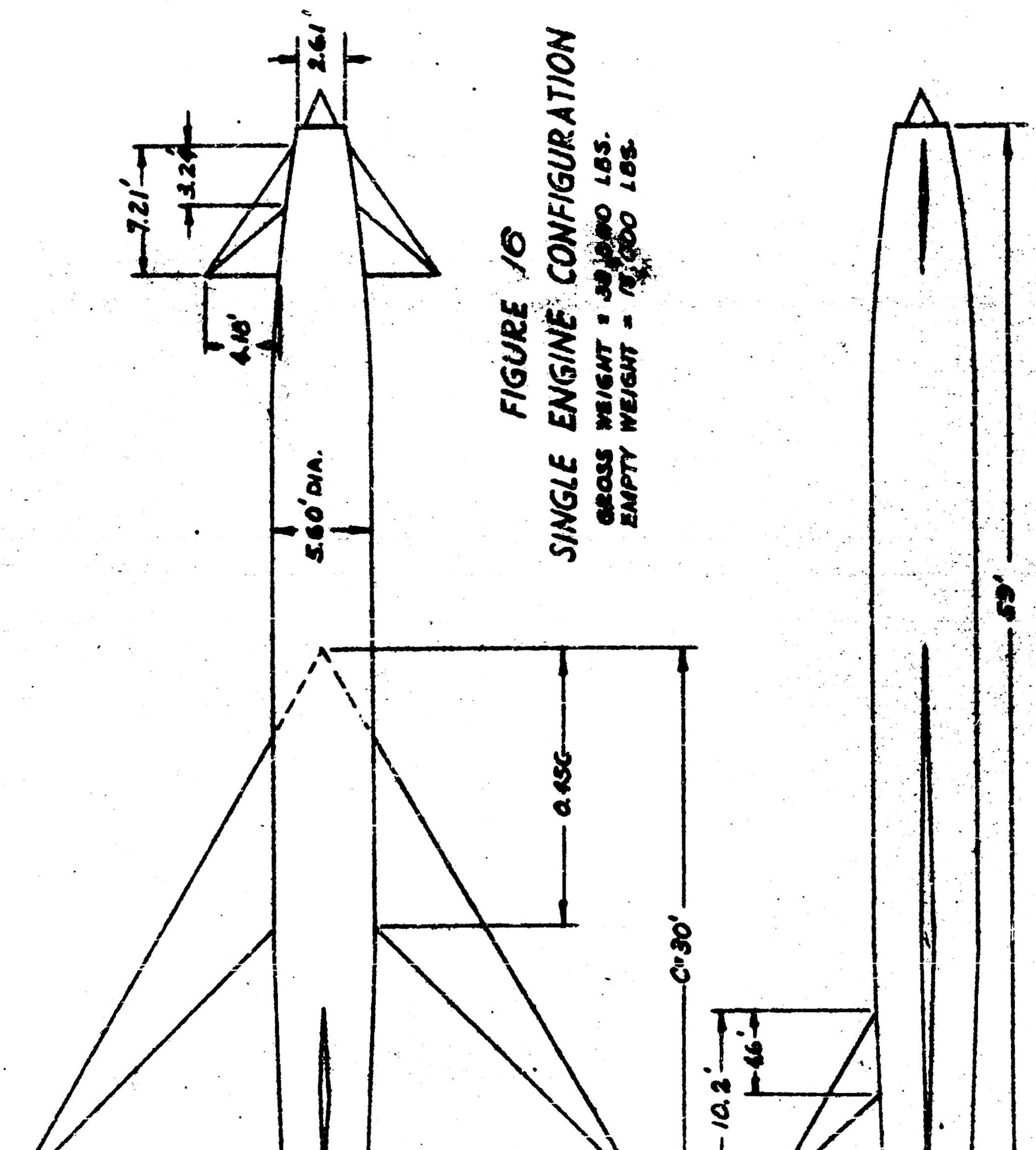

FIGURE 16
SINGLE ENGINE CONFIGURATION
GROSS WEIGHT = [illegible] LBS.
EMPTY WEIGHT = [illegible] LBS.

PREPARED BY: AP	AEROPHYSICS DEVELOPMENT CORPORATION	REPORT NO. 3002-1-R1
CHECKED BY: DG	PACIFIC PALISADES, CALIFORNIA	DATE 27 May 1953

FIGURE 17

DRAG AT ZERO LIFT
TWIN ENGINE CONFIGURATION

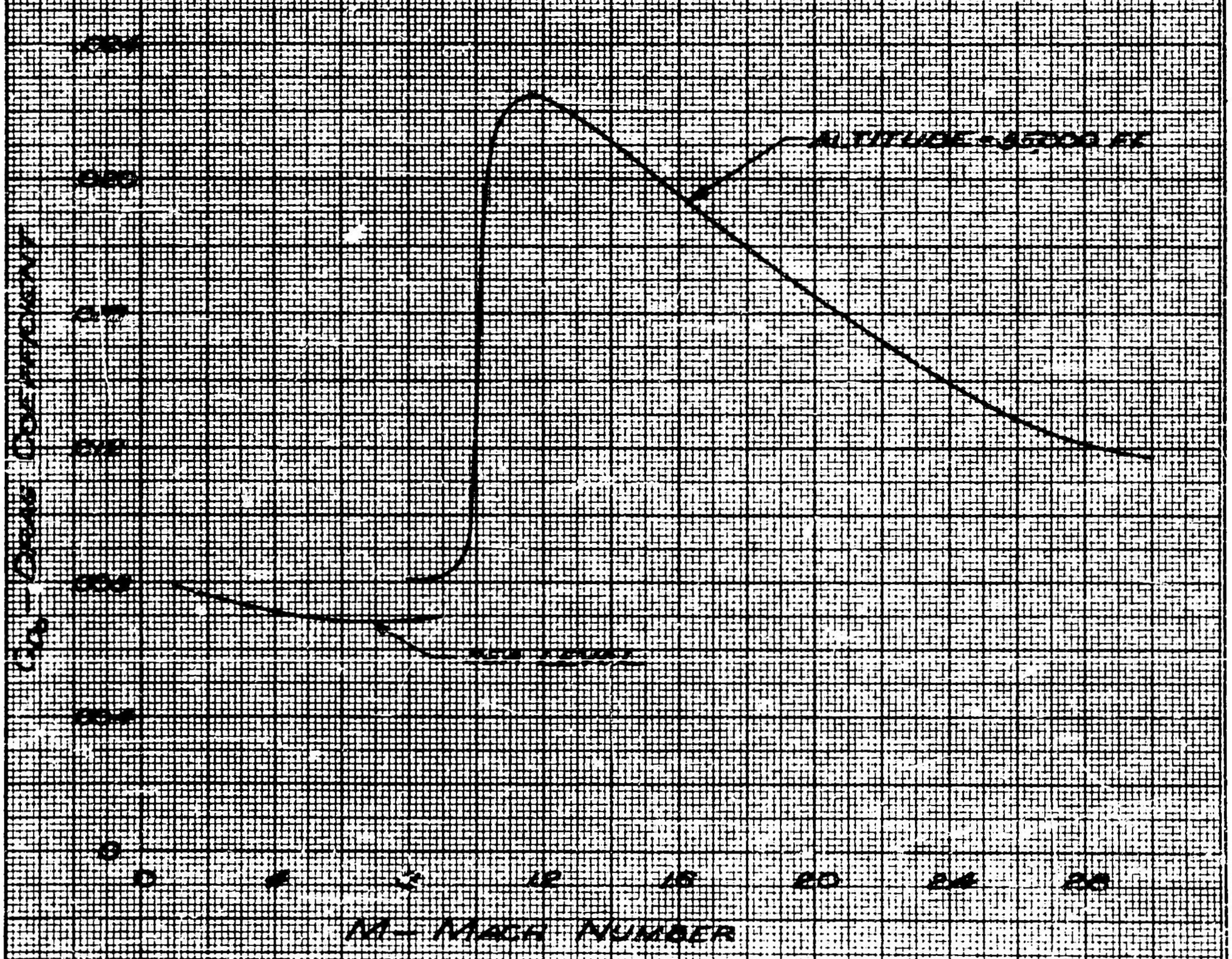

PREPARED BY: AP	AEROPHYSICS DEVELOPMENT CORPORATION	REPORT NO 3002-1-R1
CHECKED BY:	PACIFIC PALISADES, CALIFORNIA	DATE 27 May 1953

FIGURE 18

DRAG AT ZERO LIFT
SINGLE ENGINE CONFIGURATION

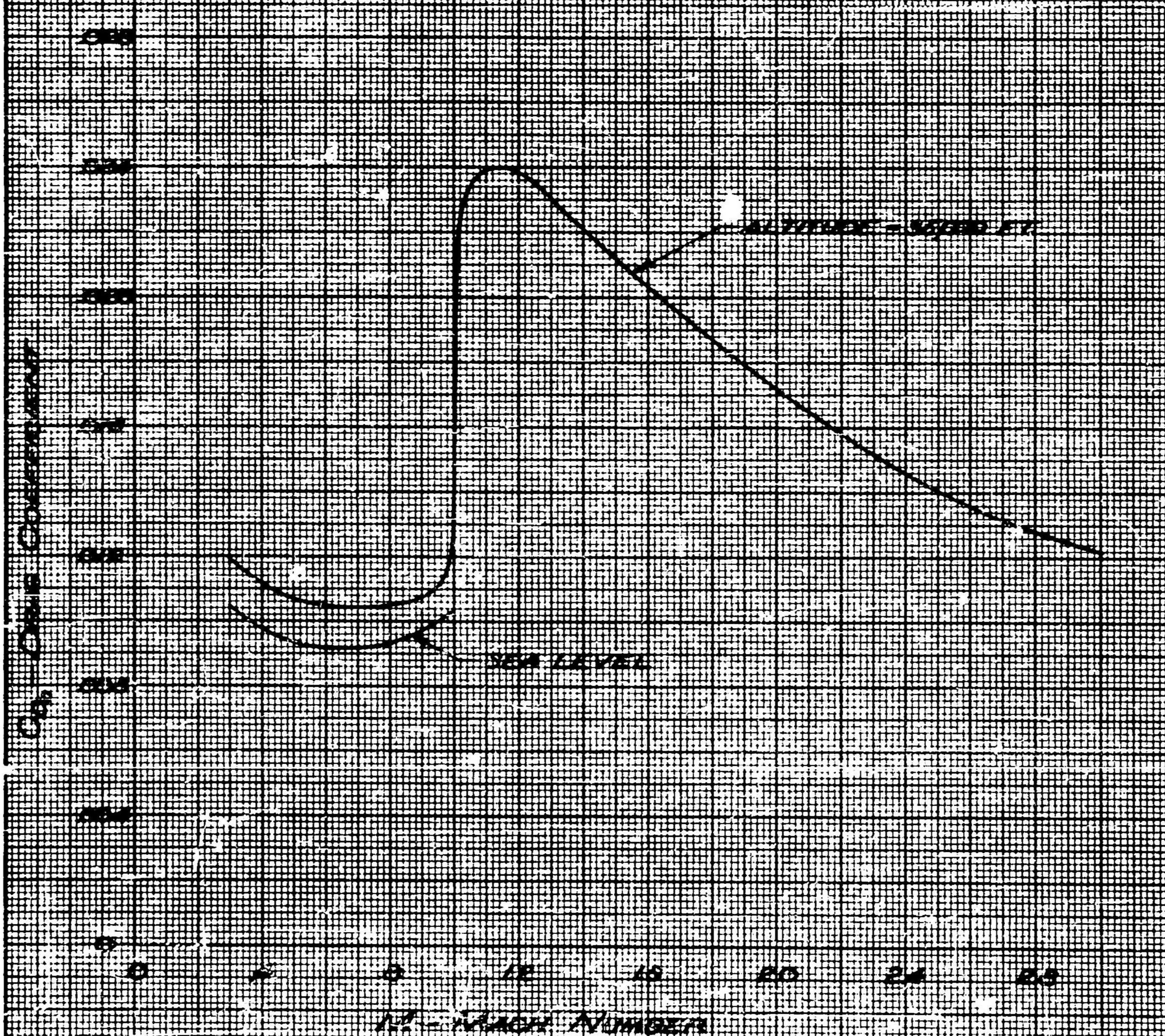

PREPARED BY: AP	AEROPHYSICS DEVELOPMENT CORPORATION	REPORT NO. 3002-1-R1
CHECKED BY: [illegible]	PACIFIC PALISADES, CALIFORNIA	DATE 27 May 1953

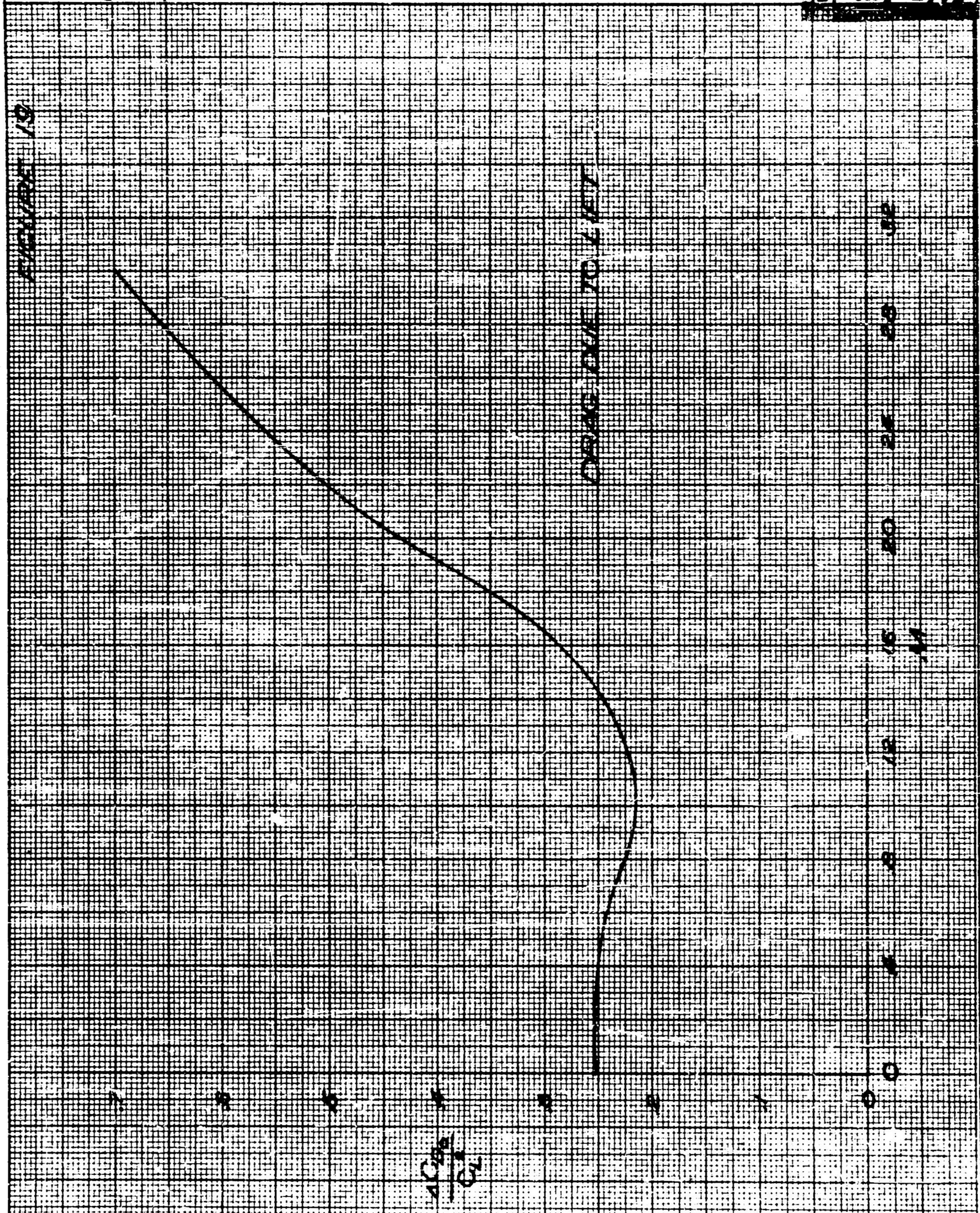

PREPARED BY: AP	AEROPHYSICS DEVELOPMENT CORPORATION	REPORT NO. 3002-1-R1
CHECKED BY:	PACIFIC PALISADES, CALIFORNIA	DATE 27 May 1953 [redacted]

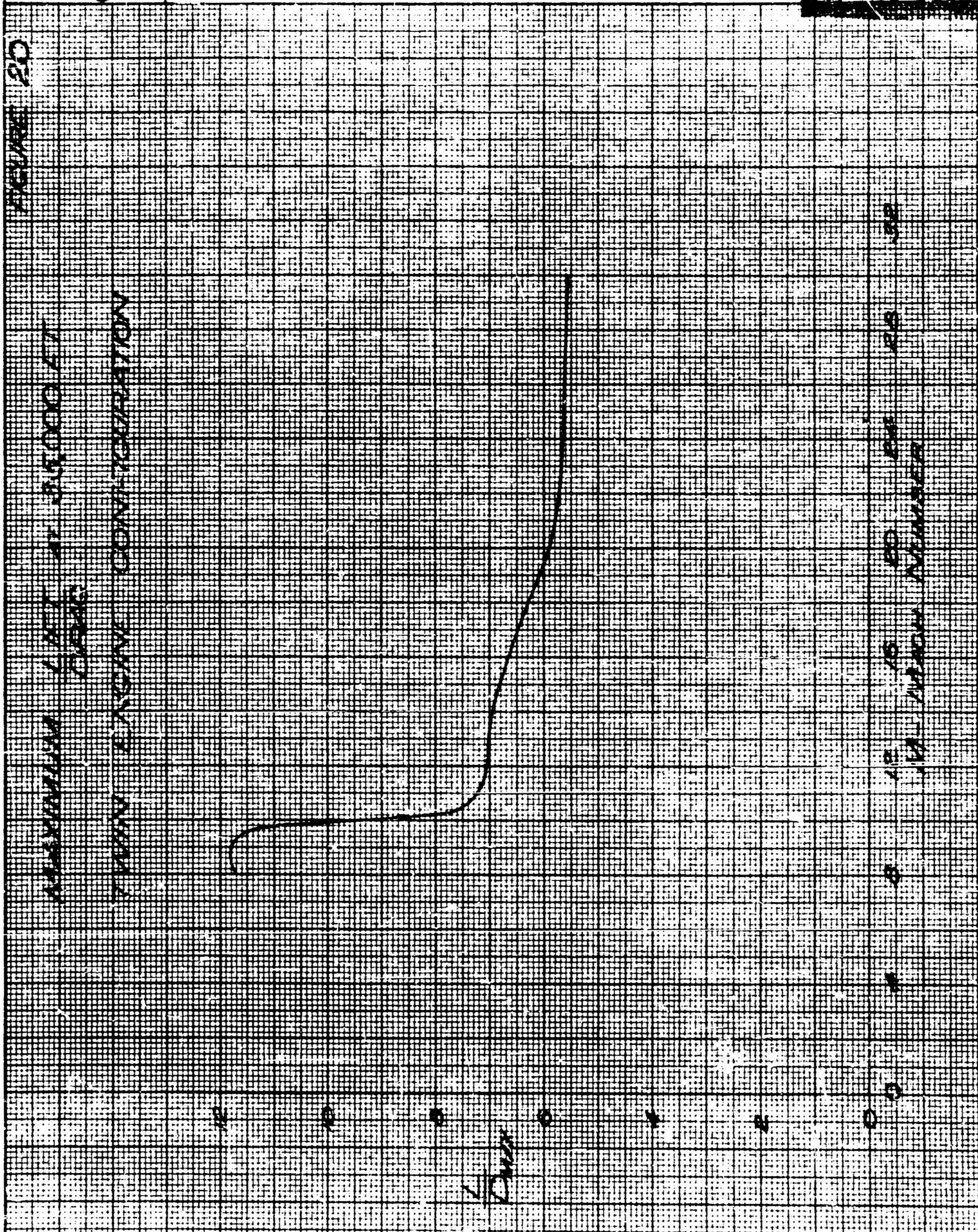

PREPARED BY: AP	AEROPHYSICS DEVELOPMENT CORPORATION	3002-1-R1
CHECKED BY: [illegible]	PACIFIC PALISADES, CALIFORNIA	DATE 27 May 1953

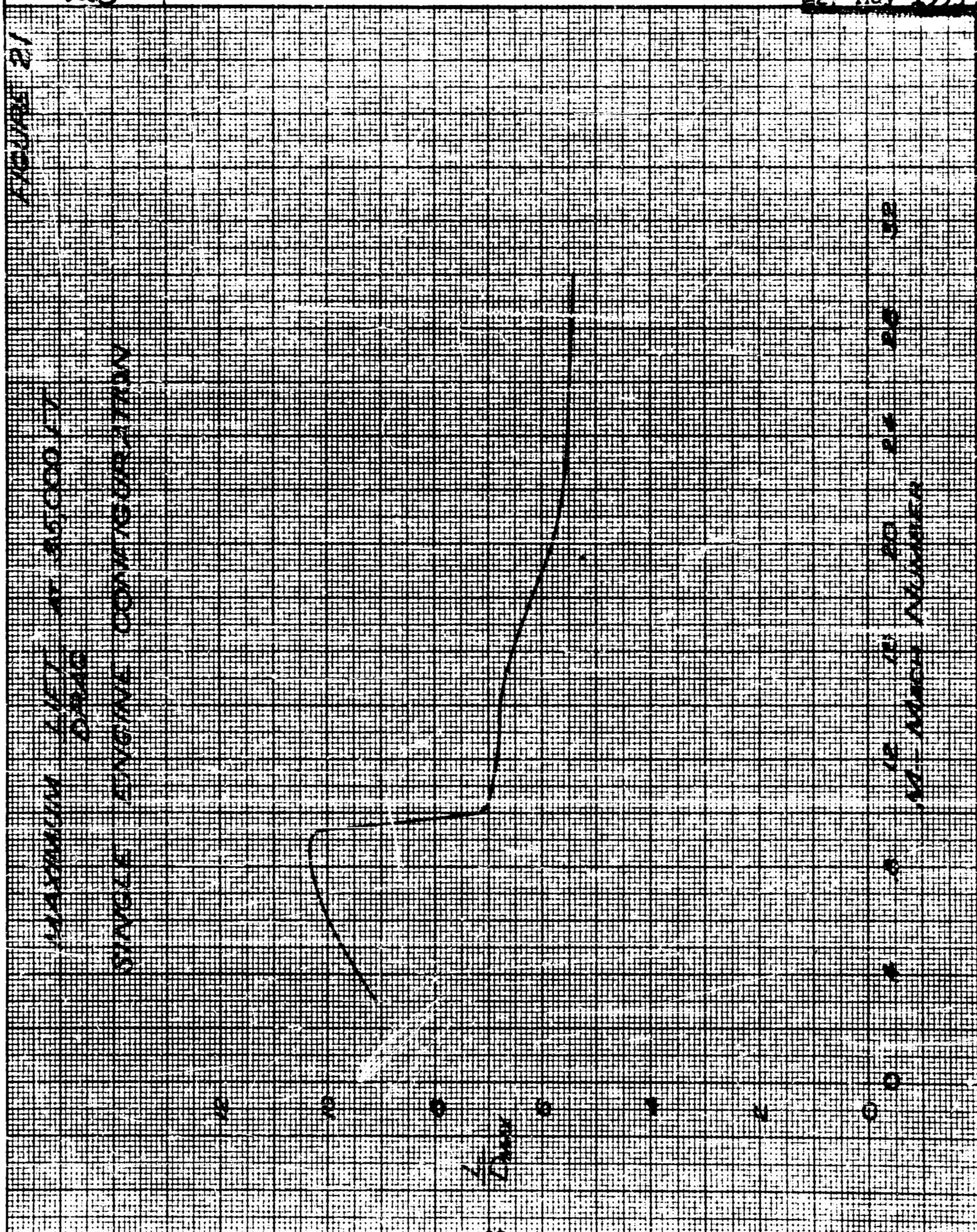

PREPARED BY: SB	AEROPHYSICS DEVELOPMENT CORPORATION	REPORT NO:
CHECKED BY:	P. O. BOX 657, PACIFIC PALISADES, CALIFORNIA	DATE: 6-19-53

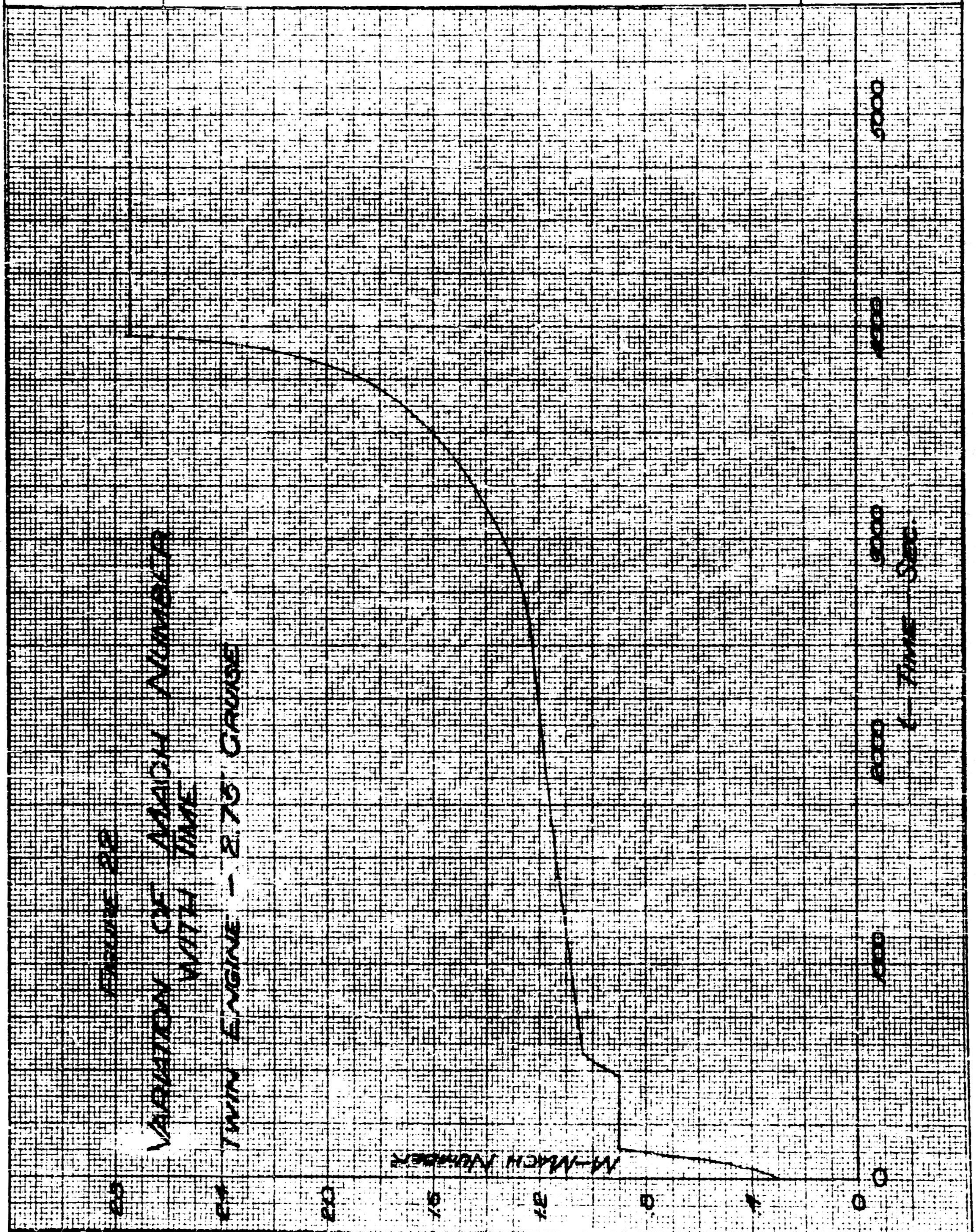

PREPARED BY: SB	AEROPHYSICS DEVELOPMENT CORPORATION	REPORT NO:
CHECKED BY:	P.O. BOX 657, PACIFIC PALISADES, CALIFORNIA	DATE: 6-19-53

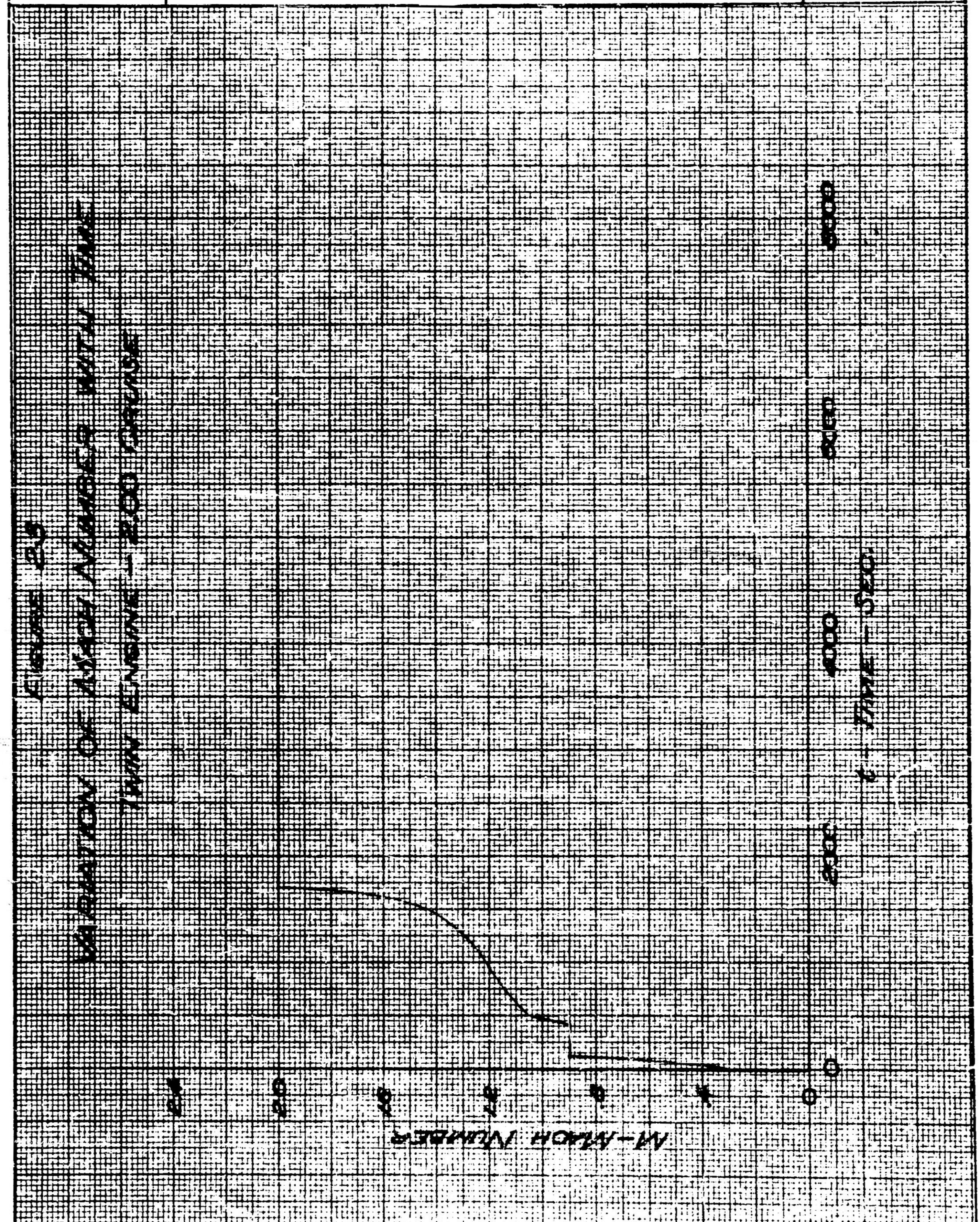

FIGURE 23
VARIATION OF MACH NUMBER WITH TIME
TWIN ENGINE - 200 CRUISE

PREPARED BY: SB	AEROPHYSICS DEVELOPMENT CORPORATION	REPORT NO:
CHECKED BY:	P. O. BOX 657, PACIFIC PALISADES, CALIFORNIA	DATE: 6-19-53.

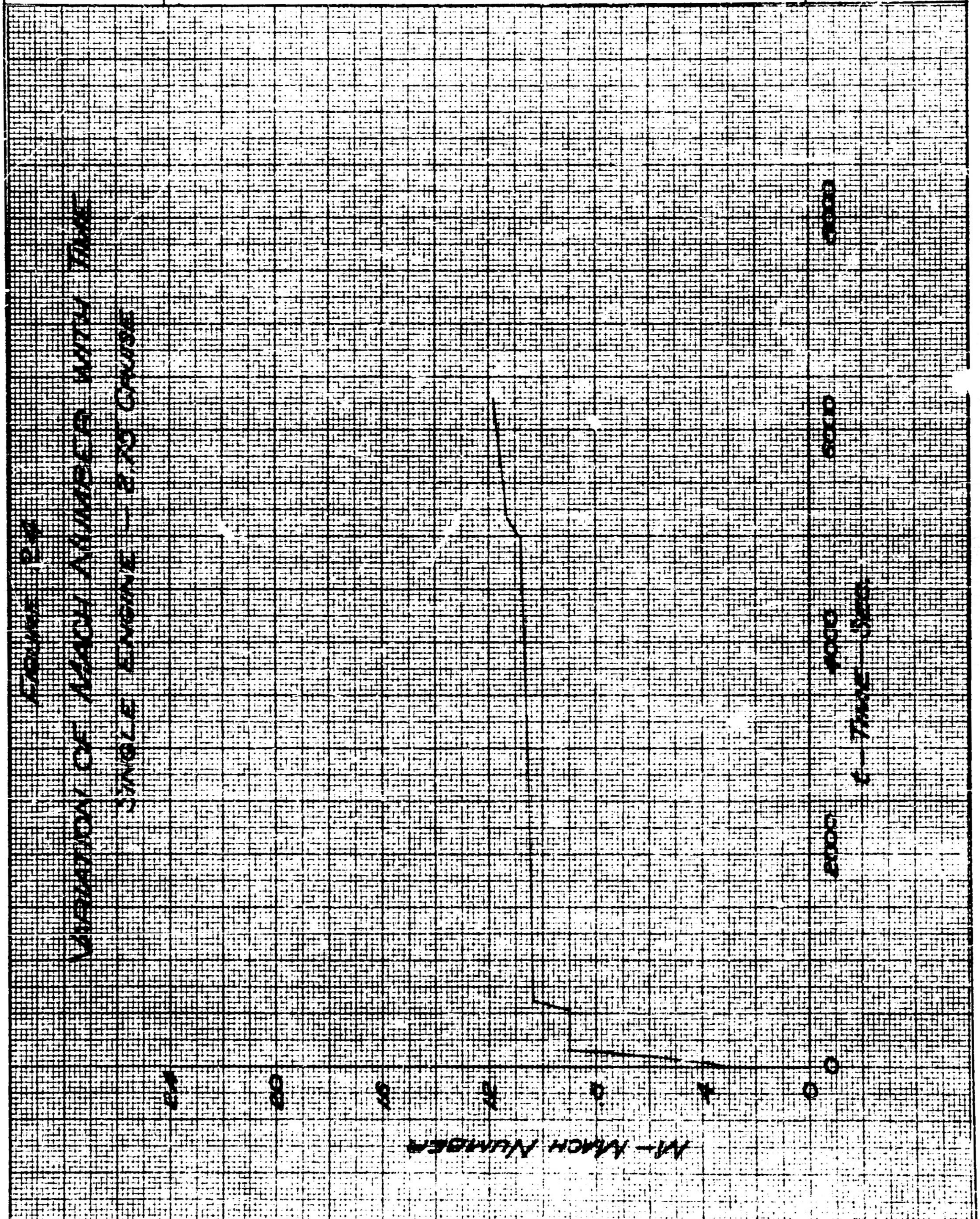

PREPARED BY: SB	AEROPHYSICS DEVELOPMENT CORPORATION	REPORT NO:
CHECKED BY:	P. O. BOX 657, PACIFIC PALISADES, CALIFORNIA	DATE: 6-19-53

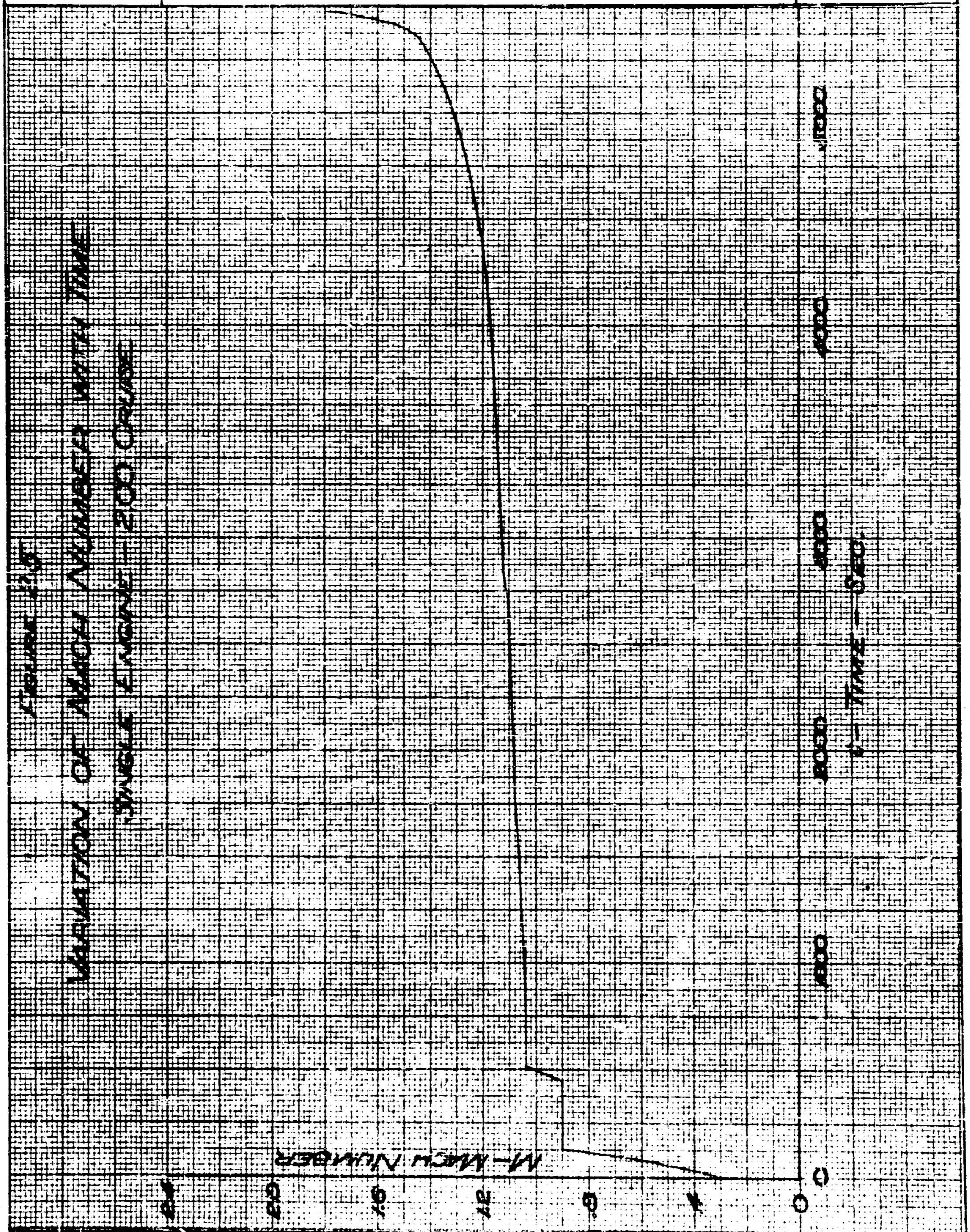

PREPARED BY: SB	AEROPHYSICS DEVELOPMENT CORPORATION	REPORT NO:
CHECKED BY:	P. O. BOX 657, PACIFIC PALISADES, CALIFORNIA	DATE: 6-19-53

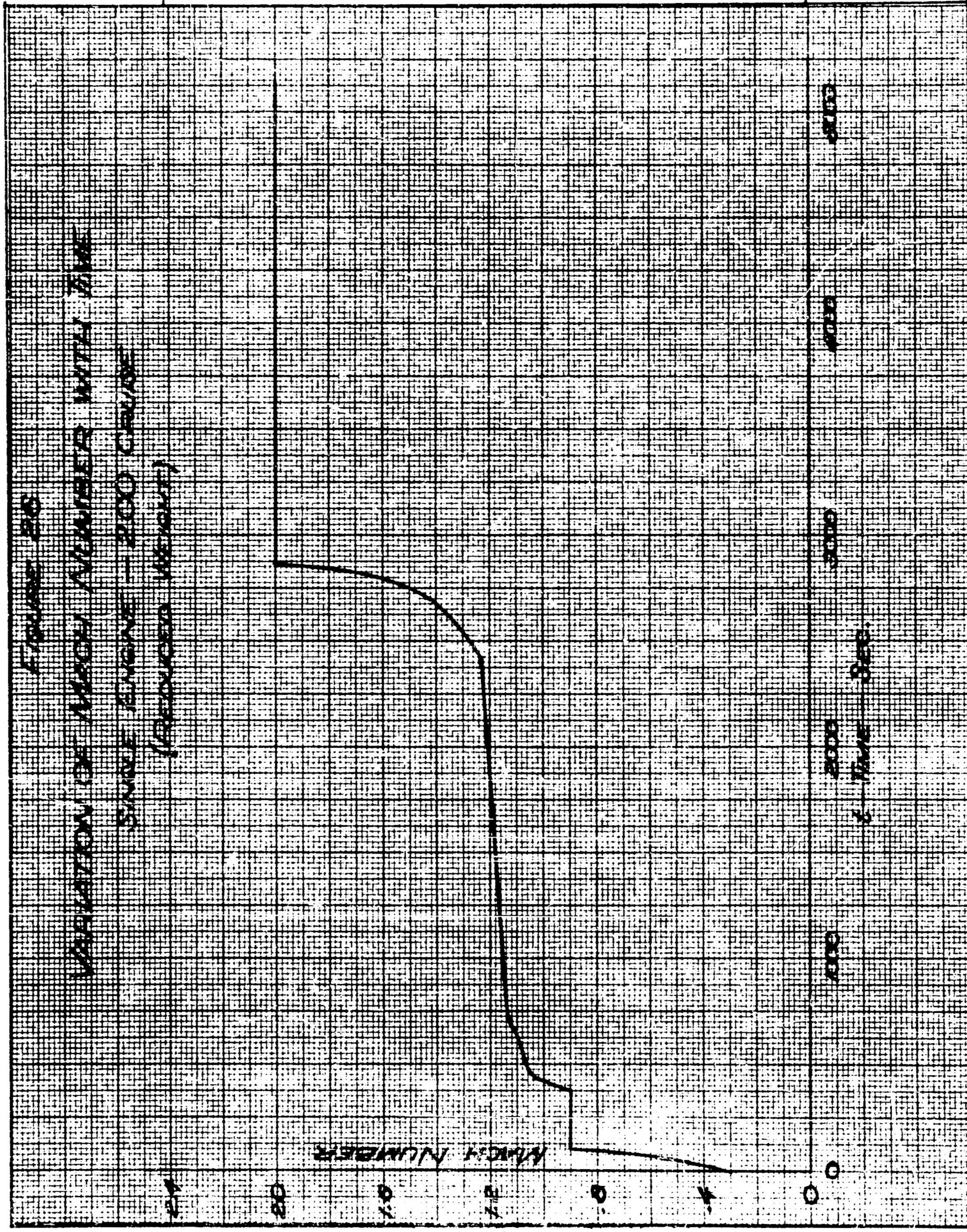

PREPARED BY: 5B & AP	AEROPHYSICS DEVELOPMENT CORPORATION	REPORT NO:
CHECKED BY:	P.O. BOX 657, PACIFIC PALISADES, CALIFORNIA	DATE: 6-19-53

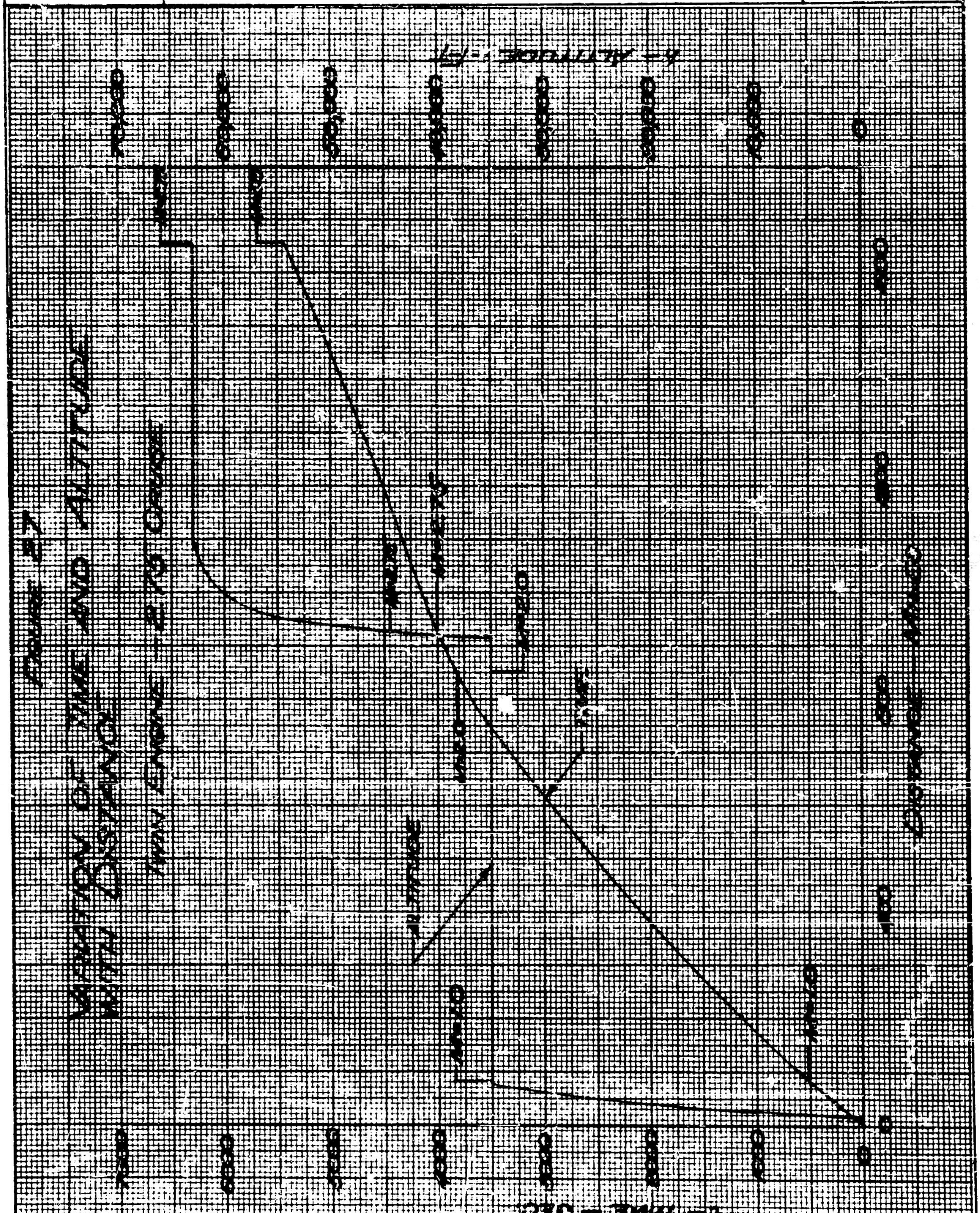

PREPARED BY: SB & AP	AEROPHYSICS DEVELOPMENT CORPORATION	REPORT NO:
CHECKED BY:	P.O. BOX 657, PACIFIC PALISADES, CALIFORNIA	DATE: 6-19-53

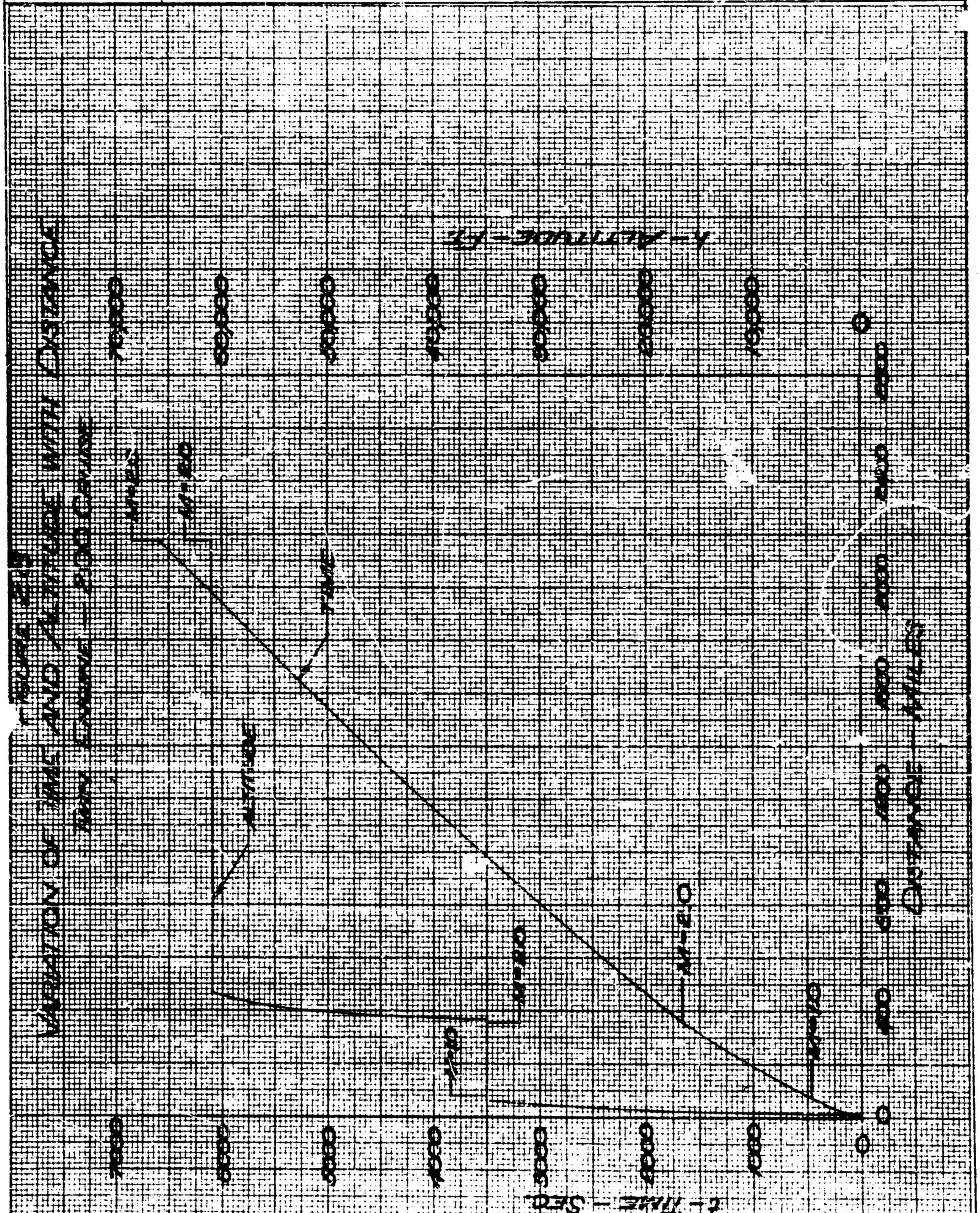

PREPARED BY: SB & AP	AEROPHYSICS DEVELOPMENT CORPORATION	REPORT NO:
CHECKED BY:	P. O. BOX 657, PACIFIC PALISADES, CALIFORNIA	DATE: 6-19-53.

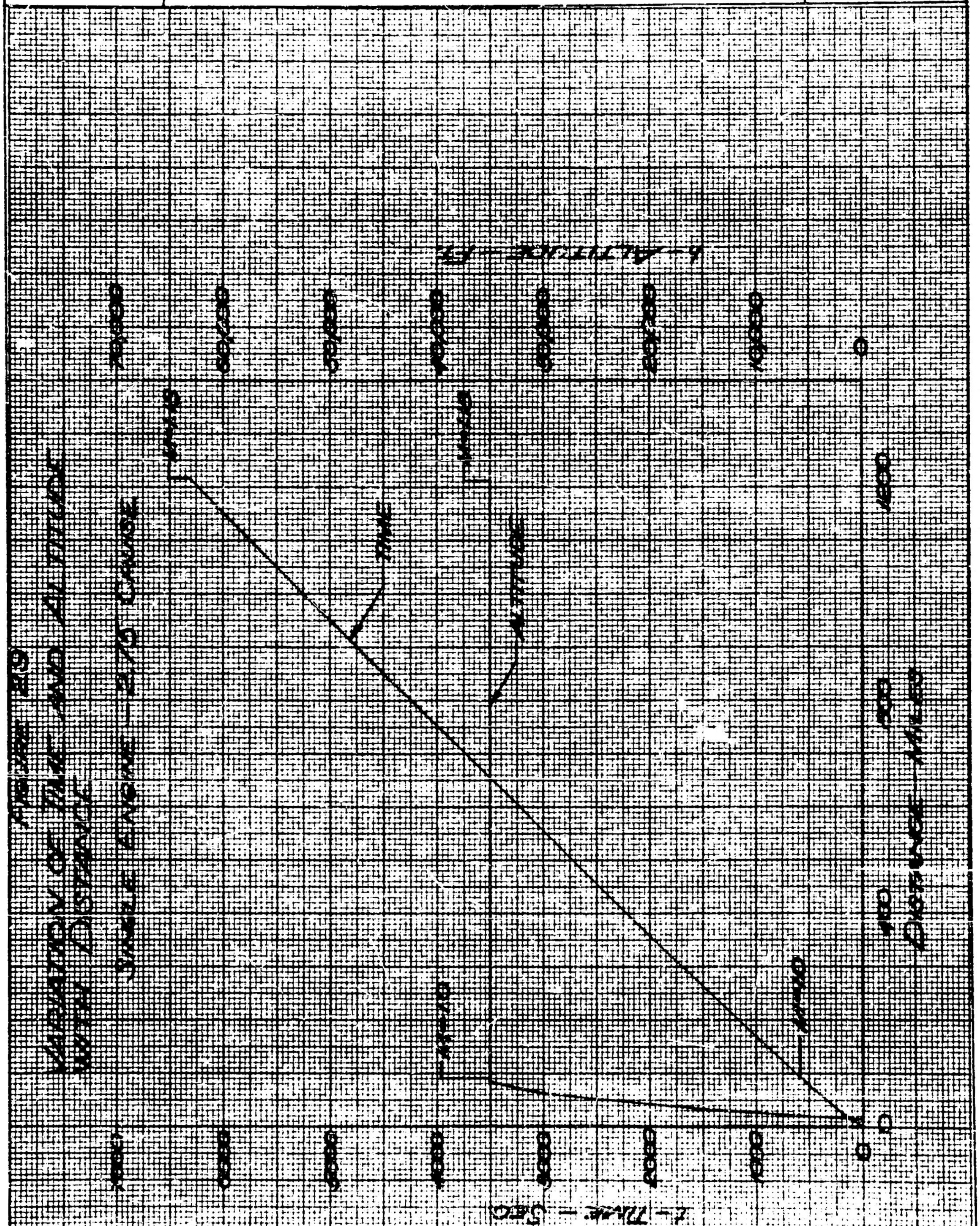

PREPARED BY: SB & AP	AEROPHYSICS DEVELOPMENT CORPORATION	REPORT NO:
CHECKED BY:	P.O. BOX 657, PACIFIC PALISADES, CALIFORNIA	DATE: 6-19-53

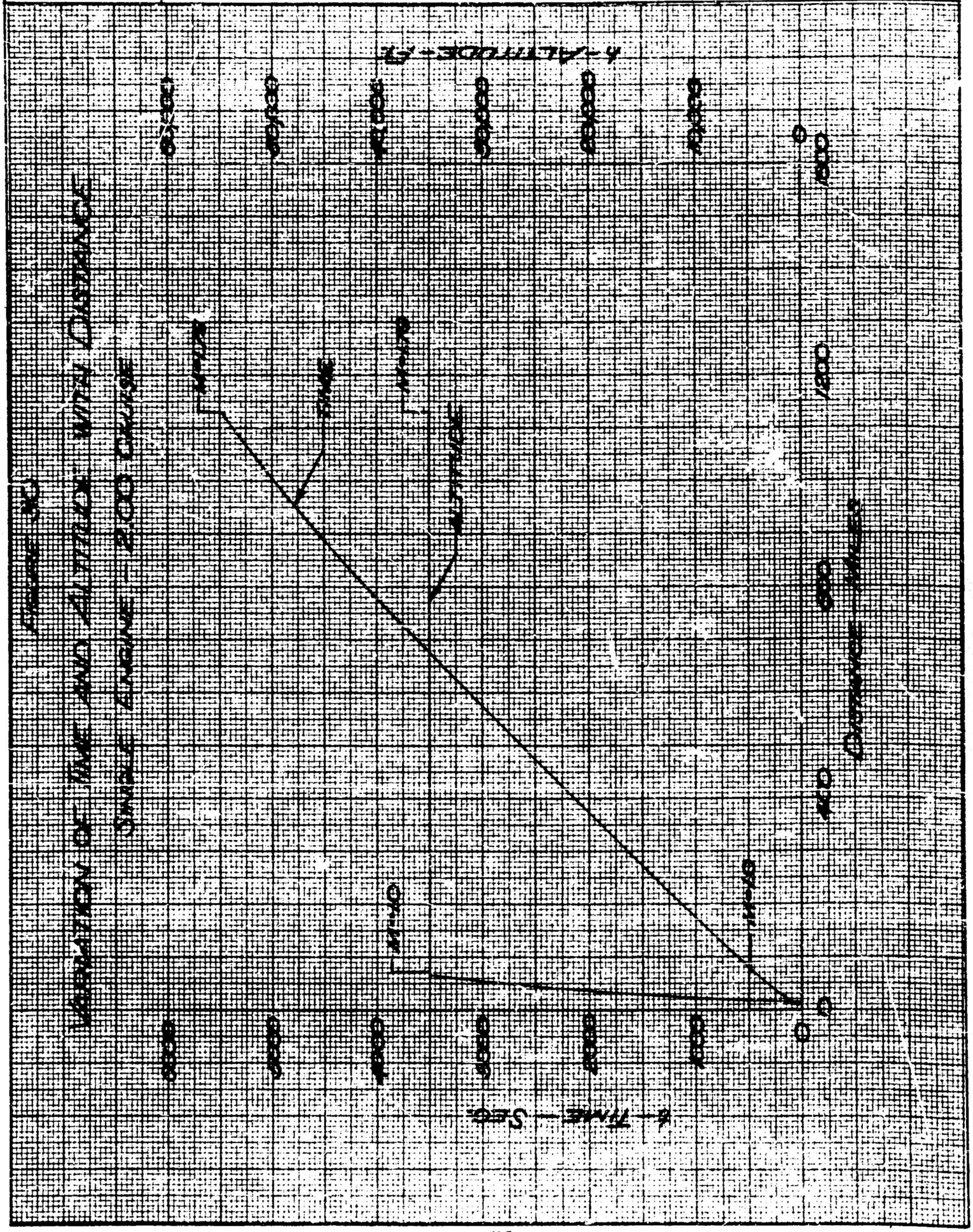

PREPARED BY: SB & AP	AEROPHYSICS DEVELOPMENT CORPORATION	REPORT NO:
CHECKED BY:	P. O. BOX 657, PACIFIC PALISADES, CALIFORNIA	DATE: 6-19-53